

1 **Alfvén waves related to moon-magnetosphere** 2 **interactions**

3 Bertrand Bonfond and Ali Sulaiman

4 **Abstract** The electro-dynamic interactions between moons and the magnetosphere
5 of their host planets have been investigated since the mid-20th century and the
6 implication of the Alfvén waves was recognized right away. However, in the first
7 models, Alfvén waves were only considered as current carriers. It is only after the
8 Voyager missions that the possibility of complex reflection patterns was considered
9 and their ability to accelerate particles became fully appreciated only recently. In
10 this chapter, we review the history of our understanding of the various cases of
11 moon-magnetosphere interactions in our Solar System. The presence of the largest
12 of these moons in the stream of the magnetospheric plasma generates powerful
13 large-scale Alfvén waves, which can break up into smaller scales, reflect off density
14 gradients and accelerate particles, ultimately impacting the atmosphere of the planet
15 to generate auroras and trigger radio emissions. The best known case is the Io-Jupiter
16 interaction, since its observational signatures are the richest and most obvious. As
17 our means of investigation improved, signatures of similar interactions have also
18 been discovered for the other Galilean moons, as well as for moons orbiting Saturn.
19 Interestingly, similar interactions can occur on rare occasions between the planets
20 themselves and the solar wind and most likely take place in exo-planetary systems
21 as well.

Bertrand Bonfond

STAR Institute, Université de Liège, Allée du Six Août, 19c, 4000 Liège, Belgium, e-mail:
b.bonfond@uliege.be

Ali Sulaiman

School of Physics and Astronomy, University of Minnesota, Minneapolis, MN, USA, e-mail: asu-
lai@umn.edu

22 **1 History of the moon-magnetosphere interactions**

23 This chapter deals with a particular type of phenomenon involving Alfvén waves
 24 throughout the Solar System: the moon-magnetosphere interactions. As we will
 25 discuss below, the motion of a moon through the magnetospheric plasma can excite
 26 powerful Alfvén waves propagating in both directions along the magnetic field lines
 27 towards the host planet and generate spectacular auroral phenomena. Furthermore,
 28 the peculiar geometries of these systems sometimes allow clear disentanglement of
 29 the different steps of the process, from the local Alfvén wave generation at the moons,
 30 to their intense signature in the radio emissions, passing through their filamentation
 31 via a turbulent cascade, their reflection at density gradients and their interaction with
 32 charged particles, making them fascinating plasma physics laboratories.

In most cases in our Solar System, the regime of the moon-magnetosphere interaction is sub-Alfvénic, i.e. the relative velocity between the incoming plasma and the obstacle v_0 is lower than the local Alfvén speed

$$v_A = \frac{B}{\sqrt{\mu_0 \rho}}$$

, where B is the magnetic field strength, μ_0 is vacuum permeability and ρ is the plasma mass density, in other words, the Alfvén Mach number

$$M_A = \frac{v_0 \sqrt{\mu_0 \rho}}{B}$$

33 , where v_0 is the relative velocity between the moon and the magnetospheric plasma,
 34 is lower than one (with the exception of Titan, our Moon, and Callisto). The nature of
 35 the interaction would not change abruptly beyond this threshold, but the amplitude
 36 of the far-field magnetic disturbance decreases rapidly as the Alfvén Mach number
 37 increases (Ridley, 2007; Sarantos and Slavin, 2009). An illustration of this transi-
 38 tion can be found on Figure 1, which shows results from a magneto-hydrodynamic
 39 simulation of the interaction between a magnetised planet and the solar wind for
 40 different Alfvén Mach numbers between 8.2 and 0.7. It can be seen that the mag-
 41 netosphere transforms into Alfvén wings, carrying more and more energy along the
 42 Z-axis (i.e. along the magnetic field lines). Saur (2021) provided a thorough review
 43 of the moon-magnetosphere interaction, with an emphasis on the theory of the local
 44 interaction. Hence, the present review is rather focused on the observations and on
 45 the way they advanced our understanding of the processes involved.

46 It is important to distinguish two types of obstacles generating Alfvén waves, the
 47 mechanical obstacles and the electromagnetic obstacles. The former can be further
 48 separated into 1) inert obstacles, for which the moon’s surface absorbs particles from
 49 the incoming plasma, generating a low density wake downstream and 2) mass-loading
 50 obstacles, for which moons with a significant atmosphere modify the momentum
 51 of the incoming plasma as the newly ionized particles drag the field lines before
 52 being accelerated. On the other hand, electromagnetic obstacles can be formed by
 53 either an intrinsic or an induced magnetic field, which can itself originate either in

54 the ionosphere, in a sub-surface ocean, in an asthenosphere (a ductile and partially
55 melted layer below a rocky crust) and in a metallic core. In practice, the effects are
56 combined, as a moon can both have an atmosphere and a sub-surface conductive
57 layer (e.g. Europa, see section 2.1.2).

58 The case of Io and Jupiter is probably the most prominent example, at least his-
59 torically speaking. The first hint of the peculiar relationship between Io and Jupiter
60 came by Bigg (1964), who noted that the decametric radio emissions from Jupiter
61 were modulated by Io's position both along its orbit and in the Jovian magnetic
62 field. At the same time, but much closer to the Earth, the first experimental telecom-
63 munication satellite, a 30 m wide balloon named Echo 1, was losing altitude at a
64 larger rate than expected. Drell et al. (1965) suggested an original theory to explain
65 this strange behavior: since Echo 1 basically consisted of a giant sphere of electri-
66 cally conductive metal, it was electro-magnetically interacting with the terrestrial
67 magnetic field. As the flux tubes filled with magnetospheric plasma move relative
68 to the spacecraft, an electric field forms across it perpendicular to both the motion
69 direction and the magnetic field. Since the body of the spacecraft is conductive, an
70 electric current would flow across the spacecraft. The Lorenz force, perpendicular to
71 both the magnetic field and the current direction would be oriented in the direction
72 opposite to Echo 1's velocity vector, would then slow the spacecraft down. At the
73 same time, the magnetic field associated with this transverse electric current would
74 shield the object from the external magnetic field. The interaction between the space-
75 craft and the surrounding plasma generates Alfvén waves, which propagate along
76 the magnetic field lines (forming structure called Alfvén wings) and which carry
77 field aligned currents, thus allowing for the current flowing across the spacecraft to
78 close outside of it.

79 While the unexpected slowing down of Echo 1 turned out to be more easily
80 explained by an underestimation of the radiation pressure and atmospheric drag
81 at its orbiting altitude, the idea of an electric current associated with motion of a
82 conductive celestial body disturbing the ambient plasma flow proved to be relevant
83 and attracted other researchers, who proposed that a similar system could be at play
84 at Io. A first scenario was drafted by Piddington and Drake (1968), followed by a
85 more detailed discussion by Goldreich and Lynden-Bell (1969). This first model is
86 called the "unipolar inductor" model. It should be noted that, while this model was
87 opposed to the "Alfvén wings" model later on, it was already clear in the authors'
88 minds that the current was carried along the magnetic field lines via Alfvén waves.
89 Furthermore, the concept of Alfvén wings was already defined by Drell et al. (1965).
90 However, in the unipolar inductor model, as the Alfvén velocity was expected to
91 be close to the speed of light because the magnetosphere plasma was expected to
92 be extremely tenuous, the Alfvén waves reflecting on the Jovian ionosphere would
93 directly fall back on Io before the satellite could move significantly along its orbit.
94 Because a feedback would get established very rapidly, the interaction could then
95 be modelled as a direct current loop. The motion of Io, considered as an infinitely
96 conductive body, across Jupiter's North-South aligned magnetic field lines, induces
97 a motional electric field oriented radially in the anti-Jovian direction and the current
98 flows in the same direction. It would then connect to the Jovian ionosphere along

99 the magnetic field lines (see figure 2). Initial speculations suggested that the current
100 would flow inside Io's interior, but later iterations (Webster et al., 1972) considered
101 that the current would rather flow as Pedersen and Hall currents in Io's ionosphere.
102 Indeed, the existence of such an ionosphere was later demonstrated through Pioneer
103 10 radio occultations (Kliore et al., 1975). One of the important characteristics of this
104 family of models is that the current intensity is essentially limited by the Pedersen
105 conductivity in Jupiter's ionosphere.

106 When Voyager 1 performed a close encounter of Io on 5 March 1972 (closest
107 distance: 20500 km), its trajectory was originally designed to cross the southern Io
108 Alfvén wing, but it only skimmed it from the upstream side (Ness et al., 1979). The
109 magnetometer however measured a disturbance of the magnetic field consistent with
110 5 MA current, a number of the same order of magnitude as the initial estimates of
111 ~ 1 MA by Goldreich and Lynden-Bell (1969). Furthermore, the Voyager probes
112 revealed evidence of Io's intense volcanism and the presence of a dense plasma torus
113 along Io's orbit. Since the Alfvén velocity is inversely proportional to the square root
114 of the mass density, the validity of the direct current hypothesis came under question,
115 because the Alfvén travel time could become longer than the time taken by Io to
116 move by its diameter in the plasma's reference frame. Neubauer (1980) expanded the
117 linear model of Drell et al. (1965) into a fully non-linear model. He noted that, in this
118 situation, the current would flow along the Alfvén characteristics, which are tilted,
119 not only relative to the unperturbed field lines, but to the perturbed field lines as well
120 (contrary to the expectations of the DC current model, see Figure 2). Moreover, the
121 non-linear Alfvén current tubes (the Alfvén wings) have a non-negligible resistance
122 and, in this theoretical frame, since there is no feedback from Jupiter's ionosphere,
123 it is this Alfvénic resistance that controls the amount of current, rather than the
124 Pedersen conductance in Jupiter's ionosphere. With the Alfvén wings being distinct
125 from the Io flux tube, the Alfvén waves' reflections on the density gradient outside
126 of the plasma torus or in Jupiter's ionosphere would end up forming a complex
127 pattern, possibly explaining the shape of the radio decametric waves spectrograms
128 (Gurnett and Goertz, 1981; Bagenal, 1983). At the same time, since Io's atmosphere
129 is the source of the plasma torus, another phenomenon in addition to the unipolar
130 inductor/mass loading mechanism was proposed as a current generator: the pick-up
131 current related to the newly ionized particles (Goertz, 1980; Cheng and Paranicas,
132 1998). As neutral atoms and molecules get ionized around Io, the electrons and ions
133 start gyrating around the magnetic field lines in opposite directions, with electrons
134 going towards Jupiter and ions away from it. Vasyliūnas (2016) however argued
135 that the pick-up currents are only transient as they are almost instantaneously (i.e.
136 on the electron-gyroperiod timescale) compensated by polarization currents. The
137 main effect generating Alfvén waves and its associated currents is due to momentum
138 exchange related to mass loading: since the newly ionized plasma is initially at rest
139 relative to the moon, it exchanges momentum with the incoming plasma and slows
140 down the resulting flow. This velocity gradient in the plasma flow results in a curl
141 of the magnetic field and thus currents. The currents are transmitted along the field
142 lines by Alfvén waves.

143 Another important discovery took place between the Voyager fly-by and arrival of
144 Galileo: the finding of the Io auroral footprint, a set of spots magnetically connected
145 to Io, which are followed by an extended tail along a contour mapping to Io's orbit
146 (Figure 3a)). Its first detection in the infrared domain (Connerney et al., 1993)
147 was followed by their observation in the ultraviolet domain with the Hubble Space
148 Telescope (Clarke et al., 1996; Prangé et al., 1996). On one hand, the existence of
149 several spots (Clarke et al., 2002; Gérard et al., 2006) clearly favoured a de-coupling
150 between Io and Jupiter's ionosphere, as the multiple spots were a prediction from
151 the Alfvén wings reflection pattern (Neubauer, 1980; Gurnett and Goertz, 1981).
152 On the other hand, the presence of a long, continuous tail left the door open for the
153 establishment of a steady state direct current loop associated with the acceleration
154 of the picked-up plasma towards corotation (Hill and Vasyliūnas, 2002; Delamere
155 et al., 2003).

156 Galileo's exploration of the Jovian system from December 1995 to September
157 2003 marked another giant leap in our understanding of the moon-magnetosphere
158 interactions. The spacecraft performed 7 flybys of Io, 9 of Europa, 6 of Ganymede
159 and 9 of Callisto, sending back a wealth of particle, magnetic field and wave data
160 documenting the interactions. For example, at Io, Galileo revealed a wake of stagnant
161 plasma (Frank et al., 1996) and intense bi-directional electron beams. This extended
162 wake of freshly ionized plasma remains quite stagnant relative to Io (Hinson et al.,
163 1998). Hence, this discovery led to the suggestion that the field lines disturbed by Io
164 may still be connected to it when the Alfvén waves bounce back, hence reviving the
165 idea of a DC current loop. Several hybrid models have then been proposed to reconcile
166 both approaches (e.g. Crary and Bagenal, 1997; Pontius, 2002); and Neubauer (1998),
167 as well as Saur (2004) argued that both theories were extreme cases of a more general
168 mixed Alfvén wings theory. At Europa, Galileo identified the induced magnetic field
169 stemming from Europa's sub-surface ocean (Kivelson et al., 2000). At Ganymede,
170 Galileo identified the presence of a mini-magnetosphere embedded within Jupiter's
171 one, owing to Ganymede's intrinsic magnetic field (Kivelson et al., 1998). At Callisto,
172 Galileo also found the signature of an induced magnetic field, even if its origin, a
173 sub-surface conductive layer or the ionosphere, remains unclear (Khurana et al.,
174 1998; Hartkorn and Saur, 2017). Almost a decade later, Cassini would provide a
175 similar wealth of information regarding the Kronian moons, with the most notable
176 example being the discovery of the neutral clouds originating from geysers on the
177 southern pole of Enceladus (Dougherty et al., 2006; Porco et al., 2006).

178 Before the discovery of the footprint emissions, most theoretical efforts concen-
179 trated on the generation of the Alfvén waves and on their propagation (Wright, 1987;
180 Wright and Southwood, 1987), but little consideration was given to their dissipation
181 and their ability to interact with particles. Indeed, in ideal magneto-hydrodynamics
182 (MHD), Alfvén waves do not develop a parallel electric field and are thus unable to
183 accelerate particles along the field lines (Lysak, 2023). In the framework reducing
184 the interaction to a direct current loop, should it concern the spots or the tail, the ac-
185 celeration of the auroral electrons is attributed to quasi-static potential drops located
186 above the Jovian ionosphere, described by the Knight relationship or a variation of
187 it adapted to Jupiter (Hill and Vasyliūnas, 2002; Ergun et al., 2006; Matsuda et al.,

2012). On the other hand, models focusing on the Alfvén waves propagation started
to account for the dispersive effects of the Alfvén waves (i.e. the kinetic and inertial
regimes), for which an alternating parallel electric field could develop and accelerate
the charged particles in the parallel direction. Crary (1997) proposed a model in
which inertial Alfvén waves would accelerate electrons along the field lines within
the torus via repeated Fermi acceleration. A decade later, Jones and Su (2008) con-
sidered both kinetic and inertial effects and concluded that inertial effects would be
much more efficient at accelerating the electrons in both directions along the field
lines outside the torus rather than inside it. Hess et al. (2010) further refined this sce-
nario and assessed the energy balance for each step leading to auroral emissions: the
power generation, the turbulent filamentation of the waves, the power transmission
through the torus boundaries, the efficiency of the electron acceleration and their
ability to finally precipitate into the atmosphere, and Hess et al. (2011) extended this
analysis to Europa and Enceladus. Their model showed that the electron acceleration
by inertial Alfvén waves at high latitude forms broadband bi-directional electrons
beams. The electrons accelerated away from Jupiter then cross the equatorial plane
close to Io (Jacobsen et al., 2010), which explains the Galileo measurements of bi-
directional electron beams during Io flybys. Part of this electron beam would remain
trapped on its field line and part of it would precipitate into the atmosphere in the
other end of the field line and generate auroral emissions. Indeed, Bonfond et al.
(2008) noted that the relative motion of the Io footprint spots and the occurrence of
a leading spot upstream of the brightest one was not compatible with a scenario only
relying on reflected Alfvén waves, but could be explained if electrons accelerated
anti-planetward in one hemisphere could precipitate in the opposite hemisphere (see
Figures 3b and 4). The brightest spot is generally associated with the main Alfvén
wing (MAW) originating directly from Io. A second spot, always located down-
stream of the first one, is associated to the first reflection of the Alfvén wing (RAW).
Its distance to the MAW spot is minimum in the northern hemisphere when Io is
close to the southern edge of the torus (Hinton et al., 2019) (Figure 4). A third spot
is associated with electrons accelerated away from Jupiter in one hemisphere and
precipitating in the opposite hemisphere (Trans-hemispheric Electron Beam - TEB
spot). Because electrons travel faster than Alfvén waves, the TEB spot is located up-
stream of the MAW spot in the northern hemisphere when Io is close to the southern
edge of the torus (see Figure 4) (Bonfond et al., 2008). The altitude of the brightness
peak is 850-900km (Bonfond, 2010) (Figure 3c) and its vertical profile suggests a
broadband energy distribution with a 1 keV mean energy. Another clue in favor of an
Alfvénic acceleration process is the broad vertical distribution of Io footprint main
spot and tail, which is only compatible with a broadband, kappa-like electron en-
ergy distribution, and not with a narrow distribution as expected from a quasi-static
potential drop (Bonfond et al., 2009; Bonfond, 2010; Bonfond et al., 2017c). The
resulting anisotropic distributions of field-aligned electrons are unstable to the gen-
eration of plasma waves, which are commonly observed on the flux tubes connected
to the Io footprint. A prominent one is the whistler-mode auroral hiss which arises
from a beam-plasma instability, undergoing wave growth via Landau resonance (e.g.
Sulaiman et al., 2020). The resulting band of frequencies obey a dispersion relation

233 such that higher frequencies propagate at larger angle to the background magnetic
234 field, enabling detection of the interaction well before and after the satellite footprint
235 flux tube is crossed (Figures 7 and 8c)). Radio waves are also generated as a result
236 of the moon-magnetosphere interaction, notably the Io Decametric Radio Emission.
237 Here, the anisotropic electron distribution drive the cyclotron maser instability from
238 which wave growth of radio waves occurs (Zarka, 1998). The generation of a free-
239 space mode as such enables moon-magnetosphere interactions to be detected from
240 very remote distances (Bigg, 1964).

241 After Galileo's close encounters providing precious data on the local interaction,
242 Juno's arrival at Jupiter in August 2016 offered a unique opportunity to explore
243 the physical processes at the polar end of the field lines. While its observations
244 confirmed the scenario inferred from remote sensing of the aurora, they also unveiled
245 unexpected results, suggesting that the story told here is not the final word on the
246 issue, as described on section 2.1.1.

247 As discussed above, most of the ideas related to the generation of Alfvén waves
248 by moon-magnetosphere interactions were motivated by observations of the Io-
249 Jupiter system. However, the subsequent exploration of other systems revealed that
250 the lessons learned at Io could essentially apply everywhere, even at Earth (see
251 section 2.4). It is also noteworthy that the modeling efforts reducing interactions to
252 direct current systems are fruitful first steps providing correct orders of magnitudes.
253 However, at some point, they proved to be oversimplifications that obscured essential
254 properties of the Alfvén waves, which turned out to be key to explain the increasingly
255 detailed observations, such as the decoupling between the Alfvén wing and the
256 satellite flux tube, or the bi-directional broadband electron acceleration (Neubauer,
257 1980; Bonfond et al., 2008, 2009; Hess et al., 2010). Similar limitations have also
258 been noted for the main auroral emissions at Jupiter (Bonfond et al., 2020).

259 **2 Moon-magnetosphere and similar interactions throughout the** 260 **Solar System**

261 **2.1 The Jovian moons**

262 **2.1.1 Io**

263 Because of the favourable combination of its intrinsic strength and relative proximity
264 to the Earth, the Io-Jupiter electro-magnetic interaction is the easiest to scientifically
265 investigate. Its signatures in the radio, infrared and ultraviolet domains radiate enough
266 energy to be observed from Earth, and Io has been visited by 2 spacecrafts (Voyager
267 1 and Galileo) and will soon be explored at close distance by Juno. The magnetic in-
268 situ field and particle observations from Voyager 1 (Acuña et al., 1981; Belcher et al.,
269 1981) and Galileo (Kivelson et al., 1996) provided signatures of the generation of
270 large scale Alfvén waves at Io. Furthermore, high frequency/small scale fluctuations

271 of the magnetic and electric fields (see Figure 5) suggested that the Alfvén waves
272 were subject to turbulent filamentation into smaller scales, which would more easily
273 allow the Alfvén waves to escape from the torus and trigger electron acceleration
274 processes outside of it (Chust et al., 2005; Hess et al., 2010). Moreover, Galileo
275 particle instruments showed the presence of bi-directional electron beams in Io’s
276 wake (Williams et al., 1996; Frank et al., 1996; Williams and Thorne, 2003; Frank
277 and Paterson, 1999) and mono-directional above Io’s poles (Mauk et al., 2001),
278 indicative of an electron acceleration process taking place close to Jupiter. After
279 their exit from the high density torus, the Alfvén waves related either to the main
280 Alfvén wing spot or to the following tail have been observed by Juno at high latitude
281 (Gershman et al., 2019; Sulaiman et al., 2020) (Figure 7). Furthermore, Alfvénic
282 Poynting fluxes in the high-latitudes were found to highly correlate with electron
283 energy fluxes and are coupled by an efficiency (10%) that is fully consistent with
284 acceleration from Alfvén wave filamentation via a turbulent cascade process (Hess
285 et al., 2010; Sulaiman et al., 2023). Juno also observed the bidirectional broadband
286 electron population (Szalay et al., 2018) expected from the models of acceleration
287 via inertial Alfvén waves (Jones and Su, 2008; Hess et al., 2010; Damiano et al.,
288 2019). The main difference between the electron populations related to the main
289 Alfvén wing spot or the tail is the energy flux, rather than the energy or the pitch
290 angle distributions (Szalay et al., 2020b). What was less expected from previous
291 theoretical studies (e.g. Hess et al., 2013a) was the finding of proton acceleration
292 along the Alfvén wing (Szalay et al., 2020c; Clark et al., 2020). Another surprise
293 was the occasional identification of a double peak in the particle flux down the tail
294 (Szalay et al., 2018) and of a split tail in the infrared images (Mura et al., 2018).

295 The Io auroral footprint is made up of at least 3 spots and an extended tail in the
296 downstream direction. The spots are approximately 850 km long, which corresponds
297 to 3-4 times the projected size of Io, <200 km wide (<2 twice the projected width
298 of Io) and 1200 km tall (full width at half maximum) (Bonfond, 2010). The relative
299 distance between the spots evolves as Io oscillates north and south of the torus
300 centrifugal equator. The UV emitted power of the different spots varies with the
301 System-III longitude of Io (System-III is a longitude system fixed with the magnetic
302 field of Jupiter). The observed brightness results from a combination of processes
303 (Bonfond et al., 2013b; Hess et al., 2013a) and the footprint may even completely
304 vanish when it crosses an auroral injection signature (Bonfond et al., 2012; Hess
305 et al., 2013b). On the other hand, Hue et al. (2019) has shown that the brightness of
306 the main spot was not affected by the collapse of Io’s atmosphere during eclipse.

307 Moreover, high resolution images of the H_3^+ auroral emissions of the footprints
308 showed that the spots were formed of sub-structures, named sub-spots, which were
309 fixed with the planet (contrary to the larger spots features which are moving with Io)
310 (Mura et al., 2018; Moirano et al., 2021).

311 In addition to the infrared and ultraviolet domain, the morphology of the Io foot-
312 print has also been observed in the visible domain (Vasavada et al., 1999; Gladstone
313 et al., 2007).

314 The precipitation of electrons into the polar atmosphere leads to a loss-cone pitch
315 angle distribution, which is susceptible to the growth of the maser-cyclotron radio

316 emission (Queinnec and Zarka, 1998; Louis et al., 2017b). In addition to the Alfvénic
317 acceleration, which is the main source of particle energization, evidence of upward
318 migrating intermittent potential structures have also been highlighted by Hess et al.
319 (2009). The recurrent formation and upward migration of these structures every 2-3
320 minutes may explain the short timescale fluctuations of the Io footprint brightness
321 (Bonfond et al., 2007, 2013b). A visual summary of the chain of processes giving
322 rise to the auroral footprints together with the related plasma and radio waves can be
323 found on Figure 6.

324 2.1.2 Europa

325 Arising mostly from the sputtering of its icy surface by magnetospheric particles,
326 the atmosphere and ionosphere of Europa are much less dense than Io's, leading to
327 a weaker plasma interaction and 20 time smaller mass loss ($\sim 50\text{kg s}^{-1}$) (Saur et al.,
328 1999; Bagenal and Dols, 2020). However, Europa is also the source of an induced
329 magnetic field, which is one of the most compelling evidence for the existence
330 of its subsurface ocean (Kivelson et al., 2000). Both effects contribute to making
331 Europa an obstacle to the stream of magnetospheric plasma and to the generation
332 of Alfvén wings (Schilling et al., 2008, e.g.). Localized sources of neutrals related
333 to cryovolcanoes (Roth et al., 2014; Jia et al., 2018; Arnold et al., 2019; Huybrighs
334 et al., 2020) could even cause smaller structure, called Alfvén winglets, within the
335 larger Alfvénic structure (Blöcker et al., 2016). Moreover, evidence for an extended
336 plasma wake, or plume, were also found in the Galileo data (Eviatar and Paranicas,
337 2005; Kurth et al., 2001; Kivelson et al., 1999).

338 Juno has also crossed the magnetic field lines connected to the Europa footprint tail
339 and intriguing differences were found, compared to the observations at Io (Allegrini
340 et al., 2020). In addition to a broadband energy distribution with a mean energy of
341 3.6 keV, a peak at an energy of ~ 2 keV was also found, suggesting that the electron
342 acceleration was at least partly electrostatic. At the Jovian end of the Alfvén wings,
343 UV auroral spots (Clarke et al., 2002; Bonfond et al., 2017b) and a downstream
344 tail are also occasionally observed (Grodent et al., 2006; Bonfond et al., 2017c).
345 High resolution images of the infrared H_3^+ emissions also showed the occasional
346 appearance of sub-dots, similarly to Io's (Moirano et al., 2021). As shown on Figure
347 3a, the UV Europa footprint is much weaker than the Io's and it is often hard to
348 identify among the surrounding auroral emissions. The identification of a second
349 spot is even rarer, and, when it could be identified, its location and motion were
350 found consistent with those of an reflected Alfvén wing (RAW) spot (Bonfond et al.,
351 2017a).

352 While the generated power is much weaker than for Io, decametric radio emissions
353 related to the Europa footprint have also been observed by Voyager 1 and Cassini
354 (Louis et al., 2017a). The interaction between Europa and the Jovian magnetosphere
355 will become the object of great scrutiny in the next decade with the arrival of two
356 dedicated spacecrafts, Europa Clipper and JUICE.

357 2.1.3 Ganymede

358 Ganymede is the largest moon of the Solar System (with a radius $R_G = 2634$ km)
359 and is the only one with its own intrinsic magnetic field, which carves a magneto-
360 sphere within Jupiter's magnetosphere (Kivelson et al., 1998). It is this 2-3 R_G -wide
361 mini-magnetosphere that forms an obstacle to the plasma flow (Neubauer, 1998;
362 Jia et al., 2008). At the front of Ganymede's magnetosphere (i.e. the upstream side
363 relative to the magnetospheric plasma flow), the magnetic field is anti-parallel to
364 Jupiter's, a configuration favourable to magnetic reconnection. The transverse elec-
365 tric potential drop across Ganymede's magnetosphere is estimated around 80 kV
366 (Zhou et al., 2020) and the total current carried along the Alfvén waves lies around
367 0.5 MA (Lavrukhin and Alexeev, 2015). This unique configuration of a nested mag-
368 netosphere creates a variety of accelerated or trapped electron populations, either
369 on closed field lines around Ganymede or between Ganymede and Jupiter (Frank
370 et al., 1997; Williams et al., 1997a,b; Williams and Mauk, 1997; Eviatar et al.,
371 2000). Furthermore, the particles energized by magnetic reconnection at the front
372 and tail of the magnetopause are the source of local electro-static and electromag-
373 netic emissions (Gurnett et al., 1996). Galileo also measured a deceleration of the
374 convective magnetospheric plasma flow to less than one third of rigid corotation,
375 which is compatible with a traversal of an Alfvén wing (Eviatar et al., 1998). At
376 high latitudes, Ganymede's auroral footprint is formed of a least two spots (Bon-
377 fond et al., 2013a) and an elongated tail (Bonfond et al., 2017c). The presence of
378 such a tail while Ganymede is not subject to any significant mass loading implies
379 that this process isn't a necessary condition for the presence of a footprint tail. It
380 favours interpretations of the auroral footprint tails implying repeated reflections of
381 Alfvén waves, as opposed to explanations involving the progressive acceleration of
382 plasma in the wake. The motion of the secondary spot suggested an origin related
383 to trans-hemispheric electron beams; an interpretation confirmed by Juno's in situ
384 measurements when crossing field lines connected to this spot (Hue et al., 2021). On
385 field lines connected to the TEB spot, Juno only detected weak currents in addition
386 to the bi-directional electron beams, contrary to measurements in the tail where sig-
387 nificant currents and strong Alfvénic activity were also found (Szalay et al., 2020a).
388 As Juno was crossing the Ganymede footprint tail, it also encountered the source
389 region of decametric radio emissions (Louis et al., 2020). In the high-resolution
390 infrared images, sub-dots, similar to those observed at Io, were also reported (Mura
391 et al., 2018). The brightness of the main spot varies according to three separate
392 timescales: several hours, tens of minutes and 2-3 minutes (Grodent et al., 2009).
393 The first one is related to the passage of Ganymede through the denser core of the
394 plasma sheet, the second probably corresponds to interactions with local plasma
395 inhomogeneities, such as plasma injections (see also Bonfond et al. (2017b)) and the
396 shortest one could correspond either to the time between subsequent reconnection
397 on Ganymede's magnetopause or to some ionospheric feedback mechanism, such as
398 the recurrent apparition of double layer structures, as documented for Io (Hess et al.,
399 2009).

400 **2.1.4 Callisto**

401 With a faint O₂, CO₂ and H₂O atmosphere and an H corona dominated by sublimation
402 rather than sputtering (Carlson, 1999; Cunningham et al., 2015; Roth et al., 2017),
403 Callisto possesses a significant conductive ionosphere generated by photo-ionization
404 (Kliore et al., 2002). A review of Callisto’s atmosphere and space environment can
405 be found in Galli et al. (2022). Signatures of an induced magnetic field, similar
406 to Europa’s, have been recorded by Galileo. It is however uncertain whether this
407 induced field arises from currents in a sub-surface conductive layer (Khurana et al.,
408 1998; Neubauer, 1998; Zimmer et al., 2000) or in the ionosphere (Hartkorn and
409 Saur, 2017). Measurements acquired during some flybys by Galileo (namely C3 and
410 C10) suggested the presence of a downstream plasma wake (or plume), while other
411 (during C22) did not lead to the same conclusion (Gurnett et al., 2000; Eviatar and
412 Paranicas, 2005). Moreover, Galileo may have encountered a field-aligned electron
413 beam in Callisto’s wake, similar to those observed at Io (Mauk and Saur, 2007).
414 Of the 4 Galilean moons, Callisto is the one generating the weakest interaction,
415 due to the lower plasma density, the weaker ambient magnetic field and the lack of
416 a large internal field (Saur et al., 2013). At the Jovian end of the field lines, two
417 tentative detections of a Callisto auroral footprint were reported by Bhattacharyya
418 et al. (2018), based on Hubble Space Telescope UV images. If the detected spots
419 do indeed correspond to a Callisto footprint, it could be as bright as Ganymede’s.
420 However, the search for this footprint with more sensitive ultraviolet and infrared
421 instruments on board the Juno spacecraft has been unfruitful so far. In conclusion,
422 while signatures of the interaction similar to those observed for the other Galilean
423 satellites are expected, their detection (of a dense wake, of electron beams, of an
424 auroral footprint) remains uncertain and the arrival of the JUICE spacecraft is thus
425 much awaited.

426 **2.2 The Kronian moons**

427 **2.2.1 Enceladus**

428 The moons of Saturn were not expected to trigger as strong electrodynamic inter-
429 actions as those of Jupiter. Indeed, the alignment of the magnetic dipole with the
430 rotation axis prevents oscillations of the local magnetic field at the moons to generate
431 strong induced fields as on Jupiter’s moons (only the orbital eccentricities and the
432 local time variations would modify the local magnetic field). Moreover, the largest
433 moon, Titan, orbits at much larger distance from the planet, both in absolute and
434 relative terms, than the Galilean moons. The other moons were deemed too small to
435 hold a sub-surface ocean or even a significant ionosphere. However, the finding of a
436 huge water ions cloud located south of Enceladus (radius: ~250 km) and originating
437 from cryo-volcanoes led to the realization that Enceladus’s environment formed a
438 much larger obstacle than originally thought (Dougherty et al., 2006; Porco et al.,

439 2006). Initial searches for the Enceladus auroral footprint with the Hubble Space
440 Telescope were unsuccessful (Wannawichian et al., 2008), but later observations of
441 the aurora from Cassini’s UVIS (UltraViolet Imaging Spectrograph) demonstrated
442 the presence of an auroral spot connected to Enceladus (Pryor et al., 2011) (Figure
443 8a)). The electrodynamic interaction between Enceladus and Saturn similarly gives
444 rise to Alfvén wings (Jia et al., 2011). The location of Enceladus’ plume in its south-
445 ern polar region leads to a north-south asymmetry in the orientation of the Alfvén
446 wings. Furthermore, the absorption of electrons by the dust in the plume yields a
447 reversal of the sign of the Hall conductivity (anti-Hall effect), as well as a reversal
448 of the sign of the B_y perturbation (i.e. the perturbation of the magnetic field along
449 the anti-Saturn/Saturn direction) in the Alfvén wing (Simon et al., 2011; Kriegel
450 et al., 2011). Moreover, Cassini’s particle instruments detected the presence of field
451 aligned ion electron beams a few Enceladus’ radii downstream of the moon. While
452 the energy flux of these beams was sufficient to generate observable auroral foot-
453 prints on Saturn, they were oriented anti-planetward, indicating that these particles
454 had been accelerated relatively close to Saturn and away from the planet, similarly
455 to the mechanism explaining the TEBs and their associated spots at Jupiter (see
456 Figure Figure 8b). Field-aligned currents and whistler-mode auroral hiss emissions
457 from the beam-plasma instability have been measured near and within the Enceladus
458 Alfvén wing (Figure 8c)), however, unlike Io, no radio emissions have been observed
459 (Gurnett et al., 2011; Sulaiman et al., 2018).

460 2.2.2 Titan

461 Titan is Saturn’s largest moon (radius: 2575 km) and has a thick and hydrocarbon-
462 rich N_2 atmosphere and a dense ionosphere, making it a significant source of plasma
463 in Saturn’s magnetosphere. However, Titan does not play the role Io plays at Jupiter,
464 because it orbits much further away from Saturn, so that it even occasionally crosses
465 the magnetopause. Hence, depending on its position in orbit around Saturn and
466 on the solar wind conditions, Titan could be located either in the plasma sheet, in
467 the magnetosphere lobes or in the magnetosheath (Rymer et al., 2009). At such
468 distances from the planet, the magnetic field is so weak that the plasma β is larger
469 than 1 (Neubauer et al., 2006). In such conditions, the dynamics of the plasma (or
470 lack thereof) takes precedence over the magnetic tension and the interacting field
471 lines get draped around the Kronian moon. Interestingly, the timescale of convection
472 of the magnetic field becomes longer than the timescale of the changes of the external
473 field and the previous magnetic field configuration thus remains ‘fossilized’ in the
474 thick ionosphere of Titan (Bertucci et al., 2008).

475 Despite the complexity of the interaction between the ever changing magneto-
476 spheric plasma (Simon et al., 2010) and Titan’s thick exosphere and ionosphere (e.g.
477 Sillanpää et al., 2007; Wei et al., 2007; Snowden et al., 2013), numerical simula-
478 tions show the systematic development of Alfvén wings connected to Titan (Kallio
479 et al., 2007; Sillanpää and Johnson, 2015). Whether these Alfvén wings trigger any
480 significant signature on Saturn remains to be demonstrated.

481 **2.2.3 Rhea**

482 Located in Saturn’s E ring, Rhea does not have any significant magnetic field nor any
483 significant plasma source, nor is it a conducting object. Yet its surface absorbs plasma
484 while the magnetic flux passes across the 1528 km wide moon. Close encounters with
485 the Cassini spacecraft showed that this wake is subject to diamagnetic currents as the
486 pressure gradients between the plasma void ($\sim 4\text{--}6 R_{Rh}$ long) and the surrounding
487 plasma distort and bend the field lines, generating Alfvén waves (Simon et al., 2012).
488 Furthermore, a more distant flyby ($102 R_{Rh}$, see Figure 9) revealed that the Alfvén
489 wings were still present far away from Rhea and that the associated currents probably
490 close in Saturn’s ionosphere (Khurana et al., 2017). Khurana et al. (2017) also argue
491 that it is the deceleration of the plasma in the wake resulting from the pressure
492 gradient rather than the diamagnetic currents themselves that generates most of the
493 Alfvénic disturbance.

494 **2.3 Triton**

495 The time variability of Neptune’s magnetic field that is intercepted by Triton is
496 especially large due to the tilt between Neptune’s magnetic and rotational axes, as
497 well as Triton’s large orbital obliquity. The resulting structure of the electrodynamic
498 interaction is highly asymmetric, with one of Triton’s Alfvén wings shown to be
499 oriented towards upstream, initiating the deflection of the incident flow farther than
500 it would otherwise (Simon et al., 2022). It is therefore reasonable to expect a highly
501 complex current system and propagation pattern of Alfvén waves, and, consequently,
502 regions where dissipation, particle acceleration, and auroral generation would take
503 place.

504 **2.4 The Earth**

505 At 1 astronomical unit (AU), the solar wind Alfvén Mach number is generally on
506 the order of 8, thus the conditions are not favourable to the formation of significant
507 Alfvén wings, as they bend over to form the magnetotail lobes (see the top left panel
508 on Figure 1). However, during the passage of an interplanetary coronal mass ejection
509 (ICME) across the Earth, the density of the solar wind can occasionally become so
510 low and the field strength so high that the interaction gets both sub-fast and sub-
511 Alfvénic. Under such atypical conditions, magneto-hydrodynamic simulations show
512 that the bow shock expands out and vanishes and well formed Alfvén wings develop
513 (Ridley, 2007) (see Figure 1). Chané et al. (2012) found observational evidence that
514 the Earth entered into such a regime for four hours between 24 and 25 May 2002.
515 During this interval, the magnetic field wasn’t unusually high (~ 9.8 nT), but the
516 estimated density dropped down to 0.05 cm^{-3} (compared to typical values between

517 0.6 to 20cm^{-3}). The Geotail spacecraft was located on the dusk side of the Earth
518 and its magnetic field and plasma velocity measurements suggest that the spacecraft
519 entered and exited the Alfvén wing 9 times. Figure 10 shows the expected shape and
520 orientation of the Alfvén wings during this time interval compared to the typical
521 shape of the terrestrial magnetosphere. Such exceptionally low density values were
522 achieved because an ICME expanded right in the wake of another one (Chané et al.,
523 2021).

524 **2.4.1 The Moon**

525 The Moon is also an inert object without any significant magnetic field or mass-
526 loading source. Moreover, the Moon orbits so far away from the Earth that it spends
527 most of its time in the super sonic and super Alfvénic interplanetary medium. And
528 yet, the two Moon orbiting ARTEMIS spacecrafts found a bending of the magnetic
529 field and a deceleration of the plasma flow in the Moon’s wake, which are interpreted
530 as characteristic signatures of Alfvén waves (Zhang et al., 2016) (see Figure 11). It is
531 however unlikely that this configuration would allow a significant amount of energy
532 and current to propagate along the magnetic field lines.

533 **2.5 Mercury**

534 Since Mercury is closer to the Sun than the Earth (perihelion:0.31 AU, aphelion:0.47
535 AU), the typical magnetic field strength, and thus the typical Alfvén Mach number
536 is also much lower than for the Earth ($\sim 2-3$ compared to ~ 8 or above for the Earth).
537 Hence Alfvén Mach number excursions below 1 during ICMEs crossings are also
538 expected to be more frequent, especially throughout the time interval for which the
539 field is strong but the density is low after the initial interplanetary shock. Using a
540 simple analytical models, Sarantos and Slavin (2009) explored the possibility for
541 the formation of Alfvén wings at Mercury with low Alfvén Mach number, since
542 Mercury, under such configurations, is expected to be an intermediate state between
543 Ganymede and the Earth. The BepiColombo may soon bring us further evidence of
544 Alfvén wings originating from Mercury.

545 **2.6 Exoplanets**

546 As discussed, the interaction between Solar System planets and the solar wind can
547 occasionally become sub-Alfvénic, allowing for the propagation of energy at large
548 distances. However, even at Mercury, the Alfvén speed remains lower than the solar
549 wind speed and these waves will never reach the solar atmosphere. Indeed, the Alfvén
550 radius, i.e. the limit inside of which the Alfvén speed is larger than the stellar wind

551 speed, is $\lesssim 0.1$ AU while Mercury orbits at least three times farther out. However,
552 an increasingly large number of exoplanets are being discovered and many of them
553 orbit at close distances relative to their parent stars, including some orbiting inside
554 the Alfvén radius, making it possible to trigger a planetary footprint on the star.
555 Furthermore, observational evidence is accumulating in favor of such Star Planet
556 Magnetic Interaction (SPMI). This evidence can be sorted into two categories: one
557 focuses on single targets and requires the monitoring of a star’s luminosity through
558 time, and the second consists of statistical investigations of anomalous stellar activity
559 on large catalogs of stars with known close-in exoplanets. In the first category,
560 the most compelling case probably concerns HD 179949, which shows surplus of
561 Ca II K chromospheric emissions synchronous with the orbital period of a know
562 exoplanet (Shkolnik et al., 2003). Other tentative evidence were reported based on
563 optical broadband photometry (Walker et al., 2008; Pagano et al., 2009) or X-ray
564 emissions (Maggio et al., 2015). Unfortunately, the statistical approach, has not
565 provided conclusive evidence yet (e.g. Viswanath et al., 2020).

566 It should be noted that the electromagnetic interaction between planets and stars
567 may be much more varied and complex than those studied in our solar system.
568 For example, the relative motion of the planet in the plasma stream is most often
569 dominated by the radial motion of the stellar wind, rather than the orbital motion
570 of the planet. Moreover, while the orientation of the stellar magnetic field may be
571 mostly latitudinal for a planet orbiting very close, it is expected to become essentially
572 longitudinal at larger distances. Then the planets and their magnetosphere may also
573 display more varied configurations (presence of conductive layers, atmospheres,
574 ionospheres and magnetospheres) compared to the moons of the Giant Planets. And
575 finally, the star’s intrinsic variability and activity certainly complicates the picture
576 and probably explains why SPMI signatures are not systematically observed, even at
577 HD 179949 (Shkolnik et al., 2008). But the most important argument to consider is
578 the fact that a stellar atmosphere is quite different than a planetary one. Indeed some
579 authors have noted that the power of the excess chromospheric emissions appeared
580 three orders of magnitude larger than the expected energy arising from the Alfvénic
581 interaction (Saur et al., 2013). This finding motivated the investigation of alternative
582 scenarios, where the SPMI would modulate the star’s emissions rather than directly
583 provide the energy. The interested reader is referred to the recent reviews by Shkolnik
584 and Llama (2018); Saur (2018) and Strugarek (2018).

585 **3 Summary**

586 The electrodynamic interaction between a plasma flow and large celestial bodies,
587 especially at low Alfvén Mach number, can generate powerful Alfvén waves propa-
588 gating energy at large distances along the magnetic field lines. But the Alfvén waves
589 generation is only the first step of a long chain of processes, including turbulence,
590 complex reflection patterns, electric currents, energy transport and dissipation, mo-
591 mentum transfer, wave-particle interaction, aurora, joule heating of the ionosphere

592 of the parent planet and powerful radio emission. Examples of similar interaction
593 abound in the Solar System, but the Jovian moons, and the Io-Jupiter interaction in
594 particular, are the best studied ones so far. Indeed, this case benefits both from a
595 low Alfvén Mach number, a strong energy generation and a relative stability of the
596 incoming plasma characteristics, which all facilitate the measurements of the signa-
597 tures of the Alfvén waves and their consequences, as well as their interpretation. For
598 other systems, the puzzle is missing more pieces, as sometimes we only have access
599 to hints of the local interaction. It is however remarkable that Alfvén wings have
600 been observed for bodies as diverse as Rhea, Io, Europa, Ganymede or the Earth.
601 Electrons beams most probably accelerated by Alfvén waves have been observed at
602 Io, Ganymede, Callisto and Enceladus, while auroral footprints have been reported
603 for all four Galilean moons and for Enceladus. Despite the idiosyncrasies associated
604 with each individual moon or planet, general patterns emerge and similar processes
605 are observed, indicating that such processes are universal and probably very common
606 in the universe. With missions specifically dedicated to the Galilean moons, such
607 as JUICE and Europa Clipper, the BebiColombo mission arriving at Mercury or a
608 future mission dedicated to the exploration of the Ice Giants, we can expect that the
609 next decade will bring us a wealth of observational clues to further complete our
610 understanding of the way Alfvén waves mediate the interaction between celestial
611 objects and the plasma flows surrounding them. Even beyond the limits of our So-
612 lar System, evidence are starting to emerge, showing the importance of the Alfvén
613 waves in the interaction between planets and their parent stars.

614 **References**

- 615 M. H. Acuña, F. M. Neubauer, and N. F. Ness. Standing Alfvén wave current system
616 at Io: Voyager 1 observations. *Journal of Geophysical Research: Space Physics*,
617 86(A10):8513–8521, 1981. ISSN 2156-2202. doi: 10.1029/JA086iA10p08513.
618 URL <https://onlinelibrary.wiley.com/doi/abs/10.1029/JA086iA10p08513>.
619 _eprint: <https://onlinelibrary.wiley.com/doi/pdf/10.1029/JA086iA10p08513>.
- 620 F. Allegrini, G. R. Gladstone, V. Hue, G. Clark, J. R. Szalay, W. S. Kurth, F. Bagenal,
621 S. Bolton, J. E. P. Connerney, R. W. Ebert, T. K. Greathouse, G. B. Hospodarsky,
622 M. Imai, P. Louarn, B. H. Mauk, D. J. McComas, J. Saur, A. H. Sulaiman,
623 P. W. Valek, and R. J. Wilson. First Report of Electron Measurements During
624 a Europa Footprint Tail Crossing by Juno. *Geophysical Research Letters*, 47
625 (18):e2020GL089732, 2020. ISSN 1944-8007. doi: 10.1029/2020GL089732.
626 URL <https://agupubs.onlinelibrary.wiley.com/doi/abs/10.1029/2020GL089732>.
627 _eprint: <https://agupubs.onlinelibrary.wiley.com/doi/pdf/10.1029/2020GL089732>.
- 628 H. Arnold, L. Liuzzo, and S. Simon. Magnetic Signatures of a Plume
629 at Europa During the Galileo E26 Flyby. *Geophysical Research Letters*,
630 46(3):1149–1157, 2019. ISSN 1944-8007. doi: 10.1029/2018GL081544.
631 URL <https://onlinelibrary.wiley.com/doi/abs/10.1029/2018GL081544>. _eprint:
632 <https://onlinelibrary.wiley.com/doi/pdf/10.1029/2018GL081544>.

- 633 F. Bagenal. Alfvén wave propagation in the Io plasma torus.
634 *Journal of Geophysical Research: Space Physics*, 88(A4):3013–3025,
635 1983. ISSN 2156-2202. doi: 10.1029/JA088iA04p03013. URL
636 <https://onlinelibrary.wiley.com/doi/abs/10.1029/JA088iA04p03013>. _eprint:
637 <https://onlinelibrary.wiley.com/doi/pdf/10.1029/JA088iA04p03013>.
- 638 F. Bagenal and V. Dols. The Space Environment of Io and Eu-
639 ropa. *Journal of Geophysical Research: Space Physics*, 125(5):
640 e2019JA027485, 2020. ISSN 2169-9402. doi: 10.1029/2019JA027485.
641 URL <https://onlinelibrary.wiley.com/doi/abs/10.1029/2019JA027485>. _eprint:
642 <https://onlinelibrary.wiley.com/doi/pdf/10.1029/2019JA027485>.
- 643 J. W. Belcher, C. K. Goertz, J. D. Sullivan, and M. H. Acuña. Plasma observations of
644 the Alfvén wave generated by Io. *Journal of Geophysical Research: Space Physics*,
645 86(A10):8508–8512, 1981. ISSN 2156-2202. doi: 10.1029/JA086iA10p08508.
646 URL <https://onlinelibrary.wiley.com/doi/abs/10.1029/JA086iA10p08508>.
647 _eprint: <https://onlinelibrary.wiley.com/doi/pdf/10.1029/JA086iA10p08508>.
- 648 C. Bertucci, N. Achilleos, M. K. Dougherty, R. Modolo, A. J. Coates, K. Szego,
649 A. Masters, Y. Ma, F. M. Neubauer, P. Garnier, J.-E. Wahlund, and D. T.
650 Young. The Magnetic Memory of Titan’s Ionized Atmosphere. *Science*,
651 321(5895):1475–1478, Sept. 2008. doi: 10.1126/science.1159780. URL
652 <https://www.science.org/doi/10.1126/science.1159780>. Publisher: American As-
653 sociation for the Advancement of Science.
- 654 D. Bhattacharyya, J. T. Clarke, J. Montgomery, B. Bonfond, J.-C. Gérard, and
655 D. Grodent. Evidence for Auroral Emissions From Callisto’s Footprint in
656 HST UV Images. *Journal of Geophysical Research: Space Physics*, 123(1):
657 364–373, Jan. 2018. ISSN 2169-9402. doi: 10.1002/2017JA024791. URL
658 <https://agupubs.onlinelibrary.wiley.com/doi/abs/10.1002/2017JA024791>.
- 659 E. K. Bigg. Influence of the Satellite Io on Jupiter’s Decametric Emission. *Nature*,
660 203(4949):1008–1010, Sept. 1964. ISSN 1476-4687. doi: 10.1038/2031008a0.
661 URL <https://www.nature.com/articles/2031008a0>.
- 662 A. Blöcker, J. Saur, and L. Roth. Europa’s plasma interaction with an
663 inhomogeneous atmosphere: Development of Alfvén winglets within the
664 Alfvén wings. *Journal of Geophysical Research: Space Physics*, 121
665 (10):9794–9828, 2016. ISSN 2169-9402. doi: 10.1002/2016JA022479.
666 URL <https://onlinelibrary.wiley.com/doi/abs/10.1002/2016JA022479>. _eprint:
667 <https://onlinelibrary.wiley.com/doi/pdf/10.1002/2016JA022479>.
- 668 B. Bonfond. The 3-D extent of the Io UV footprint on Jupiter.
669 *Journal of Geophysical Research: Space Physics*, 115(A9), Sept.
670 2010. ISSN 2156-2202. doi: 10.1029/2010JA015475. URL
671 <https://agupubs.onlinelibrary.wiley.com/doi/abs/10.1029/2010JA015475>.
- 672 B. Bonfond. When Moons Create Aurora: The Satellite Footprints on Giant Planets.
673 In *Geophysical Monograph Series*. AGU, 2012. ISBN 978-0-87590-487-0. doi:
674 10.1029/2011GM001169. URL <https://orbi.uliege.be/handle/2268/136072>.
- 675 B. Bonfond, J.-C. Gérard, D. Grodent, and J. Saur. Ultraviolet Io foot-
676 print short timescale dynamics. *Geophysical Research Letters*, 34(6),

- 677 Mar. 2007. ISSN 1944-8007. doi: 10.1029/2006GL028765. URL
678 <https://agupubs.onlinelibrary.wiley.com/doi/abs/10.1029/2006GL028765>.
- 679 B. Bonfond, D. Grodent, J.-C. Gérard, A. Radioti, J. Saur, and S. Ja-
680 cobsen. UV Io footprint leading spot: A key feature for understand-
681 ing the UV Io footprint multiplicity? *Geophysical Research Letters*, 35
682 (5), Mar. 2008. ISSN 1944-8007. doi: 10.1029/2007GL032418. URL
683 <https://agupubs.onlinelibrary.wiley.com/doi/abs/10.1029/2007GL032418>.
- 684 B. Bonfond, D. Grodent, J.-C. Gérard, A. Radioti, V. Dols, P. A. Delamere,
685 and J. T. Clarke. The Io UV footprint: Location, inter-spot distances and
686 tail vertical extent. *Journal of Geophysical Research: Space Physics*, 114
687 (A7), July 2009. ISSN 2156-2202. doi: 10.1029/2009JA014312. URL
688 <https://agupubs.onlinelibrary.wiley.com/doi/abs/10.1029/2009JA014312>.
- 689 B. Bonfond, D. Grodent, J.-C. Gérard, T. Stallard, J. T. Clarke, M. Yoneda,
690 A. Radioti, and J. Gustin. Auroral evidence of Io's control over
691 the magnetosphere of Jupiter. *Geophysical Research Letters*, 39(1),
692 Jan. 2012. ISSN 1944-8007. doi: 10.1029/2011GL050253. URL
693 <https://agupubs.onlinelibrary.wiley.com/doi/abs/10.1029/2011GL050253>.
- 694 B. Bonfond, S. Hess, F. Bagenal, J.-C. Gérard, D. Grodent, A. Ra-
695 dioti, J. Gustin, and J. T. Clarke. The multiple spots of the
696 Ganymede auroral footprint. *Geophysical Research Letters*, 40(19):4977–
697 4981, Oct. 2013a. ISSN 1944-8007. doi: 10.1002/grl.50989. URL
698 <https://agupubs.onlinelibrary.wiley.com/doi/abs/10.1002/grl.50989>.
- 699 B. Bonfond, S. Hess, J. C. Gérard, D. Grodent, A. Radioti, V. Chantry,
700 J. Saur, S. Jacobsen, and J. T. Clarke. Evolution of the Io footprint
701 brightness I: Far-UV observations. *Planetary and Space Science*, 88:64–
702 75, Nov. 2013b. ISSN 0032-0633. doi: 10.1016/j.pss.2013.05.023. URL
703 <http://www.sciencedirect.com/science/article/pii/S0032063313001402>.
- 704 B. Bonfond, G. R. Gladstone, D. Grodent, T. K. Greathouse, M. H. Versteeg,
705 V. Hue, M. W. Davis, M. F. Vogt, J.-C. Gérard, A. Radioti, S. Bolton,
706 S. M. Levin, J. E. P. Connerney, B. H. Mauk, P. Valek, A. Adriani,
707 and W. S. Kurth. Morphology of the UV aurorae Jupiter during Juno's
708 first perijove observations. *Geophysical Research Letters*, 44(10):4463–
709 4471, May 2017a. ISSN 0094-8276. doi: 10.1002/2017GL073114. URL
710 <https://agupubs.onlinelibrary.wiley.com/doi/full/10.1002/2017GL073114>.
- 711 B. Bonfond, D. Grodent, S. V. Badman, J. Saur, J. C. Gérard, and A. Radioti. Sim-
712 ilarity of the Jovian satellite footprints: Spots multiplicity and dynamics. *Icarus*,
713 292:208–217, Aug. 2017b. ISSN 0019-1035. doi: 10.1016/j.icarus.2017.01.009.
714 URL <https://www.sciencedirect.com/science/article/pii/S0019103516304547>.
- 715 B. Bonfond, J. Saur, D. Grodent, S. V. Badman, D. Bisikalo, V. Shematovich,
716 J.-C. Gérard, and A. Radioti. The tails of the satellite auroral footprints
717 at Jupiter. *Journal of Geophysical Research: Space Physics*, 122(8):7985–
718 7996, Aug. 2017c. ISSN 2169-9402. doi: 10.1002/2017JA024370. URL
719 <https://agupubs.onlinelibrary.wiley.com/doi/abs/10.1002/2017JA024370>.
- 720 B. Bonfond, Z. Yao, and D. Grodent. Six observational pieces of evidence
721 against corotation as the main cause for the aurora at Jupiter. Coperni-

- 722 cus Meetings, Aug. 2020. doi: <https://doi.org/10.5194/epsc2020-29>. URL
723 <https://meetingorganizer.copernicus.org/EPSC2020/EPSC2020-29.html>.
- 724 R. W. Carlson. A Tenuous Carbon Dioxide Atmosphere on Jupiter’s Moon Callisto.
725 *Science*, 283(5403):820–821, Feb. 1999. doi: 10.1126/science.283.5403.820.
726 URL <https://www.science.org/doi/full/10.1126/science.283.5403.820>. Publisher:
727 American Association for the Advancement of Science.
- 728 E. Chané, J. Saur, F. M. Neubauer, J. Raeder, and S. Poedts. Observational
729 evidence of Alfvén wings at the Earth. *Journal of Geophysical Research:*
730 *Space Physics*, 117(A9), 2012. ISSN 2156-2202. doi: 10.1029/2012JA017628.
731 URL <https://onlinelibrary.wiley.com/doi/abs/10.1029/2012JA017628>. _eprint:
732 <https://onlinelibrary.wiley.com/doi/pdf/10.1029/2012JA017628>.
- 733 E. Chané, B. Schmieder, S. Dasso, C. Verbeke, B. Grison, P. Démoulin, and
734 S. Poedts. Over-expansion of a coronal mass ejection generates sub-Alfvénic
735 plasma conditions in the solar wind at Earth. *Astronomy & Astrophysics*,
736 647:A149, Mar. 2021. ISSN 0004-6361, 1432-0746. doi: 10.1051/0004-
737 6361/202039867. URL [https://www.aanda.org/articles/aa/abs/2021/03/aa39867-
738 20/aa39867-20.html](https://www.aanda.org/articles/aa/abs/2021/03/aa39867-20/aa39867-20.html). Publisher: EDP Sciences.
- 739 A. F. Cheng and C. Paranicas. Model of field aligned poten-
740 tial drops near Io. *Geophysical Research Letters*, 25(6):833–
741 836, 1998. ISSN 1944-8007. doi: 10.1029/98GL00407. URL
742 <https://onlinelibrary.wiley.com/doi/abs/10.1029/98GL00407>. _eprint:
743 <https://onlinelibrary.wiley.com/doi/pdf/10.1029/98GL00407>.
- 744 T. Chust, A. Roux, W. S. Kurth, D. A. Gurnett, M. G. Kivel-
745 son, and K. K. Khurana. Are Io’s Alfvén wings filamented?
746 Galileo observations. *Planetary and Space Science*, 53(4):395–412,
747 Apr. 2005. ISSN 0032-0633. doi: 10.1016/j.pss.2004.09.021. URL
748 <http://www.sciencedirect.com/science/article/pii/S003206330400159X>.
- 749 G. Clark, B. H. Mauk, P. Kollmann, J. R. Szalay, A. H. Sulaiman, D. J.
750 Gershman, J. Saur, S. Janser, K. Garcia-Sage, T. Greathouse, C. Paranicas,
751 F. Allegrini, F. Bagenal, S. J. Bolton, J. E. P. Connerney, R. W. Ebert,
752 G. Hospodarsky, D. Haggerty, V. Hue, M. Imai, S. Kotsiaros, D. J. Mc-
753 Comas, A. Rymer, and J. Westlake. Energetic Proton Acceleration As-
754 sociated With Io’s Footprint Tail. *Geophysical Research Letters*, 47(24):
755 e2020GL090839, 2020. ISSN 1944-8007. doi: 10.1029/2020GL090839.
756 URL <https://onlinelibrary.wiley.com/doi/abs/10.1029/2020GL090839>. _eprint:
757 <https://agupubs.onlinelibrary.wiley.com/doi/pdf/10.1029/2020GL090839>.
- 758 J. T. Clarke, G. E. Ballester, J. Trauger, R. Evans, J. E. P. Connerney, K. Stapelfeldt,
759 D. Crisp, P. D. Feldman, C. J. Burrows, S. Casertano, J. S. Gallagher, R. E.
760 Griffiths, J. J. Hester, J. G. Hoessel, J. A. Holtzman, J. E. Krist, V. Meadows, J. R.
761 Mould, P. A. Scowen, A. M. Watson, and J. A. Westphal. Far-Ultraviolet Imaging
762 of Jupiter’s Aurora and the Io “Footprint”. *Science*, 274(5286):404–409, Oct.
763 1996. ISSN 0036-8075, 1095-9203. doi: 10.1126/science.274.5286.404. URL
764 <http://science.sciencemag.org/content/274/5286/404>.
- 765 J. T. Clarke, J. Ajello, G. Ballester, L. B. Jaffel, J. Connerney, J.-C. Gérard, G. R.
766 Gladstone, D. Grodent, W. Pryor, J. Trauger, and J. H. W. Jr. Ultraviolet emissions

- 767 from the magnetic footprints of Io, Ganymede and Europa on Jupiter. *Nature*,
768 415(6875):997–1000, Feb. 2002. ISSN 1476-4687. doi: 10.1038/415997a. URL
769 <https://www.nature.com/articles/415997a>.
- 770 J. E. P. Connerney, R. Baron, T. Satoh, and T. Owen. Images of Excited H_3^+ at the
771 Foot of the Io Flux Tube in Jupiter’s Atmosphere. *Science*, 262(5136):1035–1038,
772 Nov. 1993. ISSN 0036-8075, 1095-9203. doi: 10.1126/science.262.5136.1035.
773 URL <https://science.sciencemag.org/content/262/5136/1035>.
- 774 F. J. Crary. On the generation of an electron beam by Io.
775 *Journal of Geophysical Research: Space Physics*, 102(A1):37–
776 49, 1997. ISSN 2156-2202. doi: 10.1029/96JA02409. URL
777 <https://agupubs.onlinelibrary.wiley.com/doi/abs/10.1029/96JA02409>.
- 778 F. J. Crary and F. Bagenal. Coupling the plasma interaction at
779 Io to Jupiter. *Geophysical Research Letters*, 24(17):2135–2138,
780 Sept. 1997. ISSN 1944-8007. doi: 10.1029/97GL02248. URL
781 <https://agupubs.onlinelibrary.wiley.com/doi/abs/10.1029/97GL02248>.
- 782 N. J. Cunningham, J. R. Spencer, P. D. Feldman, D. F. Strobel,
783 K. France, and S. N. Osterman. Detection of Callisto’s oxygen at-
784 mosphere with the Hubble Space Telescope. *Icarus*, 254:178–189, July
785 2015. ISSN 0019-1035. doi: 10.1016/j.icarus.2015.03.021. URL
786 <https://www.sciencedirect.com/science/article/pii/S0019103515001219>.
- 787 P. A. Damiano, P. A. Delamere, B. Stauffer, C.-S. Ng, and J. R. Johnson.
788 Kinetic Simulations of Electron Acceleration by Dispersive Scale Alfvén
789 Waves in Jupiter’s Magnetosphere. *Geophysical Research Letters*, 46
790 (6):3043–3051, 2019. ISSN 1944-8007. doi: 10.1029/2018GL081219.
791 URL <https://agupubs.onlinelibrary.wiley.com/doi/abs/10.1029/2018GL081219>.
792 eprint: <https://agupubs.onlinelibrary.wiley.com/doi/pdf/10.1029/2018GL081219>.
- 793 P. A. Delamere, F. Bagenal, R. Ergun, and Y.-J. Su. Momentum transfer between
794 the Io plasma wake and Jupiter’s ionosphere. *Journal of Geophysical Research:
795 Space Physics*, 108(A6), 2003. ISSN 2156-2202. doi: 10.1029/2002JA009530.
796 URL <https://agupubs.onlinelibrary.wiley.com/doi/abs/10.1029/2002JA009530>.
- 797 M. K. Dougherty, K. K. Khurana, F. M. Neubauer, C. T. Russell, J. Saur,
798 J. S. Leisner, and M. E. Burton. Identification of a Dynamic At-
799 mosphere at Enceladus with the Cassini Magnetometer. *Science*, 311
800 (5766):1406–1409, Mar. 2006. doi: 10.1126/science.1120985. URL
801 <https://www.science.org/doi/full/10.1126/science.1120985>. Publisher: American
802 Association for the Advancement of Science.
- 803 S. D. Drell, H. M. Foley, and M. A. Ruderman. Drag and propul-
804 sion of large satellites in the ionosphere: An Alfvén propulsion en-
805 gine in space. *Journal of Geophysical Research (1896-1977)*, 70(13):
806 3131–3145, 1965. ISSN 2156-2202. doi: 10.1029/JZ070i013p03131.
807 URL <https://onlinelibrary.wiley.com/doi/abs/10.1029/JZ070i013p03131>. eprint:
808 <https://onlinelibrary.wiley.com/doi/pdf/10.1029/JZ070i013p03131>.
- 809 R. E. Ergun, Y.-J. Su, L. Andersson, F. Bagenal, P. A. Delemere, R. L.
810 Lysak, and R. J. Strangeway. S bursts and the Jupiter ionospheric
811 Alfvén resonator. *Journal of Geophysical Research: Space Physics*, 111

- 812 (A6), 2006. ISSN 2156-2202. doi: 10.1029/2005JA011253. URL
813 <https://agupubs.onlinelibrary.wiley.com/doi/abs/10.1029/2005JA011253>.
- 814 A. Eviatar and C. Paranicas. The plasma plumes of Europa and Callisto. *Icarus*, 178
815 (2):360–366, Nov. 2005. ISSN 0019-1035. doi: 10.1016/j.icarus.2005.06.007.
816 URL <https://www.sciencedirect.com/science/article/pii/S001910350500223X>.
- 817 A. Eviatar, A. F. Cheng, C. Paranicas, B. H. Mauk, R. W. McEntire, and D. J.
818 Williams. Plasma flow in the magnetosphere of Ganymede. *Geophysical Research*
819 *Letters*, 25(8):1257–1260, 1998. ISSN 1944-8007. doi: 10.1029/98GL50867.
820 URL <https://onlinelibrary.wiley.com/doi/abs/10.1029/98GL50867>.
821 eprint: <https://onlinelibrary.wiley.com/doi/pdf/10.1029/98GL50867>.
- 822 A. Eviatar, D. J. Williams, C. Paranicas, R. W. McEntire, B. H. Mauk,
823 and M. G. Kivelson. Trapped Energetic Electrons in the Magnetosphere
824 of Ganymede. *Journal of Geophysical Research: Space Physics*, 105(A3):
825 5547–5553, 2000. ISSN 2156-2202. doi: 10.1029/1999JA900450. URL
826 <https://agupubs.onlinelibrary.wiley.com/doi/abs/10.1029/1999JA900450>. eprint:
827 <https://agupubs.onlinelibrary.wiley.com/doi/pdf/10.1029/1999JA900450>.
- 828 L. A. Frank and W. R. Paterson. Intense electron beams observed at Io with the
829 Galileo spacecraft. *Journal of Geophysical Research: Space Physics*, 104(A12):
830 28657–28669, Dec. 1999. ISSN 2156-2202. doi: 10.1029/1999JA900402. URL
831 <https://agupubs.onlinelibrary.wiley.com/doi/abs/10.1029/1999JA900402>.
- 832 L. A. Frank, W. R. Paterson, K. L. Ackerson, V. M. Vasyliunas, F. V. Coroniti, and
833 S. J. Bolton. Plasma Observations at Io with the Galileo Spacecraft. *Science*,
834 274(5286):394–395, Oct. 1996. ISSN 0036-8075, 1095-9203. doi: 10.1126/sci-
835 ence.274.5286.394. URL <http://science.sciencemag.org/content/274/5286/394>.
- 836 L. A. Frank, W. R. Paterson, K. L. Ackerson, and S. J. Bolton. Low-energy electron
837 measurements at Ganymede with the Galileo spacecraft: Probes of the magnetic
838 topology. *Geophysical Research Letters*, 24(17):2159–2162, 1997. ISSN 1944-
839 8007. doi: 10.1029/97GL01632. URL
- 840 A. Galli, A. Vorburger, S. R. Carberry Mogan, E. Roussos, G. Sten-
841 berg Wieser, P. Wurz, M. Föhn, N. Krupp, M. Fränz, S. Barabash, Y. Fu-
842 taana, P. C. Brandt, P. Kollmann, D. K. Haggerty, G. H. Jones, R. E.
843 Johnson, O. J. Tucker, S. Simon, T. Tippens, and L. Liuzzo. Callisto’s
844 Atmosphere and Its Space Environment: Prospects for the Particle En-
845 vironment Package on Board JUICE. *Earth and Space Science*, 9(5):
846 e2021EA002172, 2022. ISSN 2333-5084. doi: 10.1029/2021EA002172.
847 URL <https://onlinelibrary.wiley.com/doi/abs/10.1029/2021EA002172>. eprint:
848 <https://onlinelibrary.wiley.com/doi/pdf/10.1029/2021EA002172>.
- 849 D. J. Gershman, J. E. P. Connerney, S. Kotsiaros, G. A. DiBraccio, Y. M. Martos,
850 A. F. -Viñas, V. Hue, G. Clark, F. Bagenal, S. Levin, and S. J. Bolton. Alfvénic Fluc-
851 tuations Associated With Jupiter’s Auroral Emissions. *Geophysical Research Let-
852 ters*, 46(13):7157–7165, 2019. ISSN 1944-8007. doi: 10.1029/2019GL082951.
853 URL <https://agupubs.onlinelibrary.wiley.com/doi/abs/10.1029/2019GL082951>.
854 eprint: <https://agupubs.onlinelibrary.wiley.com/doi/pdf/10.1029/2019GL082951>.
- 855 G. R. Gladstone, S. A. Stern, D. C. Slater, M. Versteeg, M. W. Davis,
856 K. D. Retherford, L. A. Young, A. J. Steffl, H. Throop, J. W. Parker,

- 857 H. A. Weaver, A. F. Cheng, G. S. Orton, J. T. Clarke, and J. D. Nichols.
858 Jupiter's Nightside Airglow and Aurora. *Science*, 318(5848):229–231, Oct.
859 2007. ISSN 0036-8075, 1095-9203. doi: 10.1126/science.1147613. URL
860 <http://science.sciencemag.org/content/318/5848/229>.
- 861 C. Goertz. Io's interaction with the plasma torus. *Journal*
862 *of Geophysical Research: Space Physics*, 85(A6):2949–2956,
863 1980. ISSN 2156-2202. doi: 10.1029/JA085iA06p02949. URL
864 <https://onlinelibrary.wiley.com/doi/abs/10.1029/JA085iA06p02949>.
865 [_eprint:
https://onlinelibrary.wiley.com/doi/pdf/10.1029/JA085iA06p02949](https://onlinelibrary.wiley.com/doi/pdf/10.1029/JA085iA06p02949).
- 866 P. Goldreich and D. Lynden-Bell. Io, a jovian unipolar inductor. *Astrophys. Journal*,
867 156:59–78, 1969.
- 868 D. Grodent, J.-C. Gérard, J. Gustin, B. H. Mauk, J. E. P. Connerney, and J. T. Clarke.
869 Europa's FUV auroral tail on Jupiter. *Geophys. Res. Lett.*, 33:6201–+, Mar. 2006.
870 doi: 10.1029/2005GL025487.
- 871 D. Grodent, B. Bonfond, A. Radioti, J.-C. Gérard, X. Jia, J. D. Nichols, and J. T.
872 Clarke. Auroral footprint of Ganymede. *Journal of Geophysical Research: Space*
873 *Physics*, 114(A7), July 2009. ISSN 2156-2202. doi: 10.1029/2009JA014289.
874 URL <https://agupubs.onlinelibrary.wiley.com/doi/abs/10.1029/2009JA014289>.
- 875 D. A. Gurnett and C. K. Goertz. Multiple Alfvén wave reflec-
876 tions excited by Io: Origin of the Jovian decametric arcs. *Journal*
877 *of Geophysical Research: Space Physics*, 86(A2):717–722,
878 1981. ISSN 2156-2202. doi: 10.1029/JA086iA02p00717. URL
879 <https://onlinelibrary.wiley.com/doi/abs/10.1029/JA086iA02p00717>.
880 [_eprint:
https://onlinelibrary.wiley.com/doi/pdf/10.1029/JA086iA02p00717](https://onlinelibrary.wiley.com/doi/pdf/10.1029/JA086iA02p00717).
- 881 D. A. Gurnett, W. S. Kurth, A. Roux, S. J. Bolton, and C. F. Kennel. Evidence
882 for a magnetosphere at Ganymede from plasma-wave observations by the Galileo
883 spacecraft. *Nature*, 384(6609):535–537, Dec. 1996. ISSN 1476-4687. doi:
884 10.1038/384535a0. URL <https://www.nature.com/articles/384535a0>. Number:
885 6609 Publisher: Nature Publishing Group.
- 886 D. A. Gurnett, A. M. Persoon, W. S. Kurth, A. Roux, and S. J.
887 Bolton. Plasma densities in the vicinity of Callisto from Galileo
888 plasma wave observations. *Geophysical Research Letters*, 27(13):
889 1867–1870, 2000. ISSN 1944-8007. doi: 10.1029/2000GL003751.
890 URL <https://onlinelibrary.wiley.com/doi/abs/10.1029/2000GL003751>.
891 [_eprint:
https://onlinelibrary.wiley.com/doi/pdf/10.1029/2000GL003751](https://onlinelibrary.wiley.com/doi/pdf/10.1029/2000GL003751).
- 892 D. A. Gurnett, T. F. Averkamp, P. Schippers, A. M. Persoon, G. B. Hospo-
893 darsky, J. S. Leisner, W. S. Kurth, G. H. Jones, A. J. Coates, F. J.
894 Crary, and M. K. Dougherty. Auroral hiss, electron beams and stand-
895 ing Alfvén wave currents near Saturn's moon Enceladus. *Geophysical Re-*
896 *search Letters*, 38(6), 2011. ISSN 1944-8007. doi: 10.1029/2011GL046854.
897 URL <https://onlinelibrary.wiley.com/doi/abs/10.1029/2011GL046854>.
898 [_eprint:
https://onlinelibrary.wiley.com/doi/pdf/10.1029/2011GL046854](https://onlinelibrary.wiley.com/doi/pdf/10.1029/2011GL046854).
- 899 J.-C. Gérard, A. Saglam, D. Grodent, and J. T. Clarke. Morphology of the ultraviolet
900 Io footprint emission and its control by Io's location. *J. Geophys. Res.*, 111(A10):
901 4202–+, 2006. doi: 10.1029/2005JA011327.

- 902 O. Hartkorn and J. Saur. Induction signals from Callisto's iono-
903 sphere and their implications on a possible subsurface ocean. *Jour-*
904 *nal of Geophysical Research: Space Physics*, 122(11):11,677–11,697,
905 2017. ISSN 2169-9402. doi: 10.1002/2017JA024269. URL
906 <https://onlinelibrary.wiley.com/doi/abs/10.1002/2017JA024269>.
907 [_eprint:
https://onlinelibrary.wiley.com/doi/pdf/10.1002/2017JA024269](https://onlinelibrary.wiley.com/doi/pdf/10.1002/2017JA024269).
- 908 S. Hess, P. Zarka, F. Mottez, and V. B. Ryabov. Electric potential jumps
909 in the Io-Jupiter flux tube. *Planetary and Space Science*, 57(1):23–
910 33, Jan. 2009. ISSN 0032-0633. doi: 10.1016/j.pss.2008.10.006. URL
911 <http://www.sciencedirect.com/science/article/pii/S0032063308003358>.
- 912 S. L. G. Hess, P. Delamere, V. Dols, B. Bonfond, and D. Swift.
913 Power transmission and particle acceleration along the Io flux
914 tube. *Journal of Geophysical Research: Space Physics*, 115(A6),
915 June 2010. ISSN 2156-2202. doi: 10.1029/2009JA014928. URL
916 <https://agupubs.onlinelibrary.wiley.com/doi/abs/10.1029/2009JA014928>.
- 917 S. L. G. Hess, P. A. Delamere, V. Dols, and L. C. Ray. Compar-
918 ative study of the power transferred from satellite-magnetosphere inter-
919 actions to auroral emissions. *Journal of Geophysical Research: Space*
920 *Physics*, 116(A1), 2011. ISSN 2156-2202. doi: 10.1029/2010JA015807.
921 URL <https://onlinelibrary.wiley.com/doi/abs/10.1029/2010JA015807>.
922 [_eprint:
https://onlinelibrary.wiley.com/doi/pdf/10.1029/2010JA015807](https://onlinelibrary.wiley.com/doi/pdf/10.1029/2010JA015807).
- 923 S. L. G. Hess, B. Bonfond, V. Chantry, J. C. Gérard, D. Grodent,
924 S. Jacobsen, and A. Radioti. Evolution of the Io footprint bright-
925 ness II: Modeling. *Planetary and Space Science*, 88:76–85, Nov.
926 2013a. ISSN 0032-0633. doi: 10.1016/j.pss.2013.08.005. URL
927 <http://www.sciencedirect.com/science/article/pii/S0032063313002109>.
- 928 S. L. G. Hess, B. Bonfond, and P. A. Delamere. How could the
929 Io footprint disappear? *Planetary and Space Science*, 89:102–110,
930 Dec. 2013b. ISSN 0032-0633. doi: 10.1016/j.pss.2013.08.014. URL
931 <http://www.sciencedirect.com/science/article/pii/S0032063313002195>.
- 932 T. W. Hill and V. M. Vasyliūnas. Jovian auroral signature of Io's corota-
933 tional wake. *Journal of Geophysical Research: Space Physics*, 107(A12):
934 SMP 27–1–SMP 27–5, 2002. ISSN 2156-2202. doi: 10.1029/2002JA009514.
935 URL <https://onlinelibrary.wiley.com/doi/abs/10.1029/2002JA009514>.
936 [_eprint:
https://onlinelibrary.wiley.com/doi/pdf/10.1029/2002JA009514](https://onlinelibrary.wiley.com/doi/pdf/10.1029/2002JA009514).
- 937 D. P. Hinson, A. J. Kliore, F. M. Flasar, J. D. Twicken, P. J. Schinder, and R. G.
938 Herrera. Galileo radio occultation measurements of Io's ionosphere and plasma
939 wake. *J. Geophys. Res.*, 103:29343–29358, 1998. doi: 10.1029/98JA02659.
- 940 P. C. Hinton, F. Bagenal, and B. Bonfond. Alfvén Wave Propagation
941 in the Io Plasma Torus. *Geophysical Research Letters*, 46(3):1242–
942 1249, 2019. ISSN 1944-8007. doi: 10.1029/2018GL081472. URL
943 <https://agupubs.onlinelibrary.wiley.com/doi/abs/10.1029/2018GL081472>.
944 [_eprint:
https://agupubs.onlinelibrary.wiley.com/doi/pdf/10.1029/2018GL081472](https://agupubs.onlinelibrary.wiley.com/doi/pdf/10.1029/2018GL081472).
- 945 V. Hue, T. K. Greathouse, B. Bonfond, J. Saur, G. R. Gladstone, L. Roth,
946 M. W. Davis, J.-C. Gérard, D. C. Grodent, J. A. Kammer, J. R. Szalay,

- 947 M. H. Versteeg, S. J. Bolton, J. E. P. Connerney, S. M. Levin, P. C. Hin-
948 ton, and F. Bagenal. Juno-UVS Observation of the Io Footprint During
949 Solar Eclipse. *Journal of Geophysical Research: Space Physics*, 124(7):
950 5184–5199, 2019. ISSN 2169-9402. doi: 10.1029/2018JA026431. URL
951 <https://agupubs.onlinelibrary.wiley.com/doi/abs/10.1029/2018JA026431>. eprint:
952 <https://agupubs.onlinelibrary.wiley.com/doi/pdf/10.1029/2018JA026431>.
- 953 V. Hue, T. K. Greathouse, G. R. Gladstone, B. Bonfond, J.-C. Gérard,
954 M. F. Vogt, D. C. Grodent, M. H. Versteeg, J. A. Kammer, G. Clark,
955 R. W. Ebert, R. S. Giles, M. W. Davis, K. Haewsantati, S. J. Bolton,
956 S. M. Levin, and J. E. P. Connerney. Detection and Characterization
957 of Circular Expanding UV-Emissions Observed in Jupiter’s Polar Auro-
958 ral Regions. *Journal of Geophysical Research: Space Physics*, 126(3):
959 e2020JA028971, 2021. ISSN 2169-9402. doi: 10.1029/2020JA028971. URL
960 <https://agupubs.onlinelibrary.wiley.com/doi/abs/10.1029/2020JA028971>. eprint:
961 <https://agupubs.onlinelibrary.wiley.com/doi/pdf/10.1029/2020JA028971>.
- 962 H. L. F. Huybrighs, E. Roussos, A. Blöcker, N. Krupp, Y. Futaana, S. Barabash,
963 L. Z. Hadid, M. K. G. Holmberg, O. Lomax, and O. Witasse. An Ac-
964 tive Plume Eruption on Europa During Galileo Flyby E26 as Indicated
965 by Energetic Proton Depletions. *Geophysical Research Letters*, 47(10):
966 e2020GL087806, 2020. ISSN 1944-8007. doi: 10.1029/2020GL087806.
967 URL <https://onlinelibrary.wiley.com/doi/abs/10.1029/2020GL087806>. eprint:
968 <https://onlinelibrary.wiley.com/doi/pdf/10.1029/2020GL087806>.
- 969 S. Jacobsen, J. Saur, F. M. Neubauer, B. Bonfond, J.-C. Gérard, and D. Grodent.
970 Location and spatial shape of electron beams in Io’s wake. *J. Geophys. Res.*, 115
971 (A14):A04205, 2010. doi: 10.1029/2009JA014753.
- 972 X. Jia, R. J. Walker, M. G. Kivelson, K. K. Khurana, and J. A. Linker. Three-
973 dimensional MHD simulations of Ganymede’s magnetosphere. *J. Geophys. Res.*,
974 113(A12):6212–+, 2008. doi: 10.1029/2007JA012748.
- 975 X. Jia, M. G. Kivelson, K. K. Khurana, and W. S. Kurth. Evidence of a plume on
976 Europa from Galileo magnetic and plasma wave signatures. *Nature Astronomy*,
977 2(6):459–464, June 2018. ISSN 2397-3366. doi: 10.1038/s41550-018-0450-z.
978 URL <https://www.nature.com/articles/s41550-018-0450-z>. Number: 6 Publisher:
979 Nature Publishing Group.
- 980 Y.-D. Jia, C. T. Russell, K. K. Khurana, H. Y. Wei, Y. J. Ma, J. S.
981 Leisner, A. M. Persoon, and M. K. Dougherty. Cassini magnetome-
982 ter observations over the Enceladus poles. *Geophysical Research Let-
983 ters*, 38(19), 2011. ISSN 1944-8007. doi: 10.1029/2011GL049013.
984 URL <https://onlinelibrary.wiley.com/doi/abs/10.1029/2011GL049013>. eprint:
985 <https://onlinelibrary.wiley.com/doi/pdf/10.1029/2011GL049013>.
- 986 S. T. Jones and Y.-J. Su. Role of dispersive Alfvén waves in generating parallel
987 electric fields along the Io-Jupiter fluxtube. *J. Geophys. Res.*, 113(A12):12205–+,
988 2008. doi: 10.1029/2008JA013512.
- 989 E. Kallio, I. Sillanpää, R. Jarvinen, P. Janhunen, M. Dougherty, C. Bertucci,
990 and F. Neubauer. Morphology of the magnetic field near Titan: Hy-
991 brid model study of the Cassini T9 flyby. *Geophysical Research Let-*

- 992 *ters*, 34(24), 2007. ISSN 1944-8007. doi: 10.1029/2007GL030827.
993 URL <https://onlinelibrary.wiley.com/doi/abs/10.1029/2007GL030827>. _eprint:
994 <https://onlinelibrary.wiley.com/doi/pdf/10.1029/2007GL030827>.
- 995 K. K. Khurana, M. G. Kivelson, D. J. Stevenson, G. Schubert, C. T. Russell, R. J.
996 Walker, and C. Polanskey. Induced magnetic fields as evidence for subsurface
997 oceans in Europa and Callisto. *Nature*, 395(6704):777–780, Oct. 1998. ISSN
998 1476-4687. doi: 10.1038/27394. URL <https://www.nature.com/articles/27394>.
999 Number: 6704 Publisher: Nature Publishing Group.
- 1000 K. K. Khurana, S. Fatemi, J. Lindkvist, E. Roussos, N. Krupp, M. Holmström, C. T.
1001 Russell, and M. K. Dougherty. The role of plasma slowdown in the genera-
1002 tion of Rhea’s Alfvén wings. *Journal of Geophysical Research: Space Physics*,
1003 122(2):1778–1788, 2017. ISSN 2169-9402. doi: 10.1002/2016JA023595.
1004 URL <https://onlinelibrary.wiley.com/doi/abs/10.1002/2016JA023595>. _eprint:
1005 <https://onlinelibrary.wiley.com/doi/pdf/10.1002/2016JA023595>.
- 1006 M. G. Kivelson, K. K. Khurana, R. J. Walker, C. T. Russell, J. A.
1007 Linker, D. J. Southwood, and C. Polanskey. A Magnetic Signature
1008 at Io: Initial Report from the Galileo Magnetometer. *Science*, 273
1009 (5273):337–340, July 1996. doi: 10.1126/science.273.5273.337. URL
1010 <https://www.science.org/doi/10.1126/science.273.5273.337>. Publisher: Ameri-
1011 can Association for the Advancement of Science.
- 1012 M. G. Kivelson, J. Warnecke, L. Bennett, S. Joy, K. K. Khurana, J. A. Linker,
1013 C. T. Russell, R. J. Walker, and C. Polanskey. Ganymede’s magnetosphere:
1014 Magnetometer overview. *Journal of Geophysical Research: Planets*, 103(E9):
1015 19963–19972, 1998. ISSN 2156-2202. doi: 10.1029/98JE00227. URL
1016 <https://agupubs.onlinelibrary.wiley.com/doi/abs/10.1029/98JE00227>. _eprint:
1017 <https://agupubs.onlinelibrary.wiley.com/doi/pdf/10.1029/98JE00227>.
- 1018 M. G. Kivelson, K. K. Khurana, D. J. Stevenson, L. Bennett, S. Joy, C. T. Russell,
1019 R. J. Walker, C. Zimmer, and C. Polanskey. Europa and Callisto: Induced or
1020 intrinsic fields in a periodically varying plasma environment. *J. Geophys. Res.*,
1021 104:4609–4626, Mar. 1999. doi: 10.1029/1998JA900095.
- 1022 M. G. Kivelson, K. K. Khurana, C. T. Russell, M. Volwerk, R. J.
1023 Walker, and C. Zimmer. Galileo Magnetometer Measurements: A
1024 Stronger Case for a Subsurface Ocean at Europa. *Science*, 289(5483):
1025 1340–1343, Aug. 2000. doi: 10.1126/science.289.5483.1340. URL
1026 <https://www.science.org/doi/10.1126/science.289.5483.1340>. Publisher: Ameri-
1027 can Association for the Advancement of Science.
- 1028 M. G. Kivelson, F. Bagenal, W. S. Kurth, F. M. Neubauer, C. Paranicas, and
1029 J. Saur. Magnetospheric interactions with satellites. pages 513–536. *Jupiter.*
1030 *The Planet, Satellites and Magnetosphere*, 2004. Citation Key Alias: kivelson-
1031 MagnetosphericInteractionsSatellites.
- 1032 A. J. Kliore, G. Fjeldbo, B. L. Seidel, D. N. Sweetnam, T. T. Sesplaukis,
1033 P. M. Woiceshyn, and S. I. Rasool. The atmosphere of Io from Pi-
1034 oneer 10 radio occultation measurements. *Icarus*, 24(4):407–410, Apr.
1035 1975. ISSN 0019-1035. doi: 10.1016/0019-1035(75)90057-3. URL
1036 <https://www.sciencedirect.com/science/article/pii/0019103575900573>.

- 1037 A. J. Kliore, A. Anabtawi, R. G. Herrera, S. W. Asmar, A. F. Nagy, D. P. Hin-
1038 son, and F. M. Flasar. Ionosphere of Callisto from Galileo radio occulta-
1039 tion observations. *Journal of Geophysical Research: Space Physics*, 107(A11):
1040 SIA 19–1–SIA 19–7, 2002. ISSN 2156-2202. doi: 10.1029/2002JA009365.
1041 URL <https://onlinelibrary.wiley.com/doi/abs/10.1029/2002JA009365>.
1042 [_eprint:
https://onlinelibrary.wiley.com/doi/pdf/10.1029/2002JA009365](https://onlinelibrary.wiley.com/doi/pdf/10.1029/2002JA009365).
- 1043 H. Kriegel, S. Simon, U. Motschmann, J. Saur, F. M. Neubauer, A. M. Per-
1044 soon, M. K. Dougherty, and D. A. Gurnett. Influence of negatively charged
1045 plume grains on the structure of Enceladus’ Alfvén wings: Hybrid simula-
1046 tions versus Cassini Magnetometer data. *Journal of Geophysical Research:*
1047 *Space Physics*, 116(A10), 2011. ISSN 2156-2202. doi: 10.1029/2011JA016842.
1048 URL <https://onlinelibrary.wiley.com/doi/abs/10.1029/2011JA016842>.
1049 [_eprint:
https://onlinelibrary.wiley.com/doi/pdf/10.1029/2011JA016842](https://onlinelibrary.wiley.com/doi/pdf/10.1029/2011JA016842).
- 1050 W. S. Kurth, D. A. Gurnett, A. M. Persoon, A. Roux, S. J. Bolton, and C. J. Alexander.
1051 The plasma wave environment of Europa. *Planetary and Space Science*, 49(3):
1052 345–363, Mar. 2001. ISSN 0032-0633. doi: 10.1016/S0032-0633(00)00156-2.
1053 URL <https://www.sciencedirect.com/science/article/pii/S0032063300001562>.
- 1054 A. S. Lavrukhin and I. I. Alexeev. Aurora at high latitudes
1055 of Ganymede. *Astronomy Letters*, 41(11):687–692, Nov. 2015.
1056 ISSN 1562-6873. doi: 10.1134/S1063773715110043. URL
1057 <https://doi.org/10.1134/S1063773715110043>.
- 1058 C. K. Louis, L. Lamy, P. Zarka, B. Cecconi, and S. L. G. Hess. Detection of
1059 Jupiter decametric emissions controlled by Europa and Ganymede with Voy-
1060 ager/PRA and Cassini/RPWS. *Journal of Geophysical Research: Space Physics*,
1061 122(9):9228–9247, 2017a. ISSN 2169-9402. doi: 10.1002/2016JA023779. URL
1062 <https://agupubs.onlinelibrary.wiley.com/doi/abs/10.1002/2016JA023779>.
1063 [_eprint:
https://agupubs.onlinelibrary.wiley.com/doi/pdf/10.1002/2016JA023779](https://agupubs.onlinelibrary.wiley.com/doi/pdf/10.1002/2016JA023779).
- 1064 C. K. Louis, L. Lamy, P. Zarka, B. Cecconi, M. Imai, W. S. Kurth,
1065 G. Hospodarsky, S. L. G. Hess, X. Bonnin, S. Bolton, J. E. P. Conner-
1066 ney, and S. M. Levin. Io-Jupiter decametric arcs observed by Juno/Waves
1067 compared to ExPRES simulations. *Geophysical Research Letters*, 44
1068 (18):9225–9232, 2017b. ISSN 1944-8007. doi: 10.1002/2017GL073036.
1069 URL <https://onlinelibrary.wiley.com/doi/abs/10.1002/2017GL073036>.
1070 [_eprint:
https://onlinelibrary.wiley.com/doi/pdf/10.1002/2017GL073036](https://onlinelibrary.wiley.com/doi/pdf/10.1002/2017GL073036).
- 1071 C. K. Louis, P. Louarn, F. Allegrini, W. S. Kurth, and J. R. Szalay. Ganymede-
1072 Induced Decametric Radio Emission: In Situ Observations and Measure-
1073 ments by Juno. *Geophysical Research Letters*, 47(20):e2020GL090021,
1074 2020. ISSN 1944-8007. doi: <https://doi.org/10.1029/2020GL090021>. URL
1075 <https://agupubs.onlinelibrary.wiley.com/doi/abs/10.1029/2020GL090021>.
1076 [_eprint:
https://agupubs.onlinelibrary.wiley.com/doi/pdf/10.1029/2020GL090021](https://agupubs.onlinelibrary.wiley.com/doi/pdf/10.1029/2020GL090021).
- 1077 R. L. Lysak. Kinetic Alfvén waves and auroral particle acceleration: a review.
1078 *Reviews of Modern Plasma Physics*, 7(1):6, Jan. 2023. ISSN 2367-3192. doi:
1079 10.1007/s41614-022-00111-2. URL [https://doi.org/10.1007/s41614-022-00111-](https://doi.org/10.1007/s41614-022-00111-2)
1080 [2](https://doi.org/10.1007/s41614-022-00111-2).

- 1081 A. Maggio, I. Pillitteri, G. Scandariato, A. F. Lanza, S. Sciortino, F. Borsa, A. S.
1082 Bonomo, R. Claudi, E. Covino, S. Desidera, R. Gratton, G. Micela, I. Pagano,
1083 G. Piotto, A. Sozzetti, R. Cosentino, and J. Maldonado. COORDINATED X-RAY
1084 AND OPTICAL OBSERVATIONS OF STAR–PLANET INTERACTION IN HD
1085 17156. *The Astrophysical Journal Letters*, 811(1):L2, Sept. 2015. ISSN 2041-
1086 8205. doi: 10.1088/2041-8205/811/1/L2. URL [https://dx.doi.org/10.1088/2041-
1087 8205/811/1/L2](https://dx.doi.org/10.1088/2041-8205/811/1/L2). Publisher: The American Astronomical Society.
- 1088 K. Matsuda, N. Terada, Y. Katoh, and H. Misawa. A simulation study of the current-
1089 voltage relationship of the Io tail aurora. *Journal of Geophysical Research (Space
1090 Physics)*, 117(A16):10214, Oct. 2012. doi: 10.1029/2012JA017790.
- 1091 B. H. Mauk and J. Saur. Equatorial electron beams and auroral structuring at Jupiter.
1092 *J. Geophys. Res.*, 112(A11):10221–+, Oct. 2007. doi: 10.1029/2007JA012370.
- 1093 B. H. Mauk, D. J. Williams, and A. Eviatar. Understanding Io’s space
1094 environment interaction: Recent energetic electron measurements from
1095 Galileo. *Journal of Geophysical Research: Space Physics*, 106(A11):
1096 26195–26208, 2001. ISSN 2156-2202. doi: 10.1029/2000JA002508.
1097 URL <https://onlinelibrary.wiley.com/doi/abs/10.1029/2000JA002508>.
1098 eprint: <https://onlinelibrary.wiley.com/doi/pdf/10.1029/2000JA002508>.
- 1099 A. Moirano, A. Mura, A. Adriani, V. Dols, B. Bonfond, J. H. Waite, V. Hue, J. R. Sza-
1100 lay, A. H. Sulaiman, B. M. Dinelli, F. Tosi, F. Altieri, A. Cicchetti, G. Filacchione,
1101 D. Grassi, A. Migliorini, M. L. Moriconi, R. Noschese, G. Piccioni, R. Sordini,
1102 D. Turrini, C. Plainaki, G. Sindoni, S. Massetti, R. L. Lysak, S. L. Ivanovski,
1103 and S. J. Bolton. Morphology of the Auroral Tail of Io, Europa, and Ganymede
1104 From JIRAM L-Band Imager. *Journal of Geophysical Research: Space Physics*,
1105 126(9):e2021JA029450, 2021. ISSN 2169-9402. doi: 10.1029/2021JA029450.
1106 URL <https://onlinelibrary.wiley.com/doi/abs/10.1029/2021JA029450>.
1107 eprint: <https://onlinelibrary.wiley.com/doi/pdf/10.1029/2021JA029450> tex.ids=
1108 moiranoMorphologyAuroralTail.
- 1109 A. Mura, A. Adriani, J. E. P. Connerney, S. Bolton, F. Altieri, F. Bagenal, B. Bonfond,
1110 B. M. Dinelli, J.-C. Gérard, T. Greathouse, D. Grodent, S. Levin, B. Mauk,
1111 M. L. Moriconi, J. Saur, J. H. Waite, M. Amoroso, A. Cicchetti, F. Fabiano,
1112 G. Filacchione, D. Grassi, A. Migliorini, R. Noschese, A. Olivieri, G. Piccioni,
1113 C. Plainaki, G. Sindoni, R. Sordini, F. Tosi, and D. Turrini. Juno observations of
1114 spot structures and a split tail in Io-induced aurorae on Jupiter. *Science*, 361(6404):
1115 774–777, Aug. 2018. ISSN 0036-8075, 1095-9203. doi: 10.1126/science.aat1450.
1116 URL <http://science.sciencemag.org/content/361/6404/774>.
- 1117 N. F. Ness, M. H. Acuña, R. P. Lepping, L. F. Burlaga, K. W. Behannon, and F. M.
1118 Neubauer. Magnetic Field Studies at Jupiter by Voyager 1: Preliminary Results.
1119 *Science*, 204(4396):982–987, June 1979. doi: 10.1126/science.204.4396.982.
1120 URL <https://www.science.org/doi/abs/10.1126/science.204.4396.982>. Publisher:
1121 American Association for the Advancement of Science.
- 1122 F. Neubauer. Nonlinear standing Alfvén wave current system at Io: The-
1123 ory. *Journal of Geophysical Research: Space Physics*, 85(A3):1171–
1124 1178, 1980. ISSN 2156-2202. doi: 10.1029/JA085iA03p01171. URL

- 1125 <https://onlinelibrary.wiley.com/doi/abs/10.1029/JA085iA03p01171>. _eprint:
1126 <https://onlinelibrary.wiley.com/doi/pdf/10.1029/JA085iA03p01171>.
- 1127 F. M. Neubauer. The sub-Alfvénic interaction of the Galilean satellites with
1128 the Jovian magnetosphere. *Journal of Geophysical Research: Planets*, 103
1129 (E9):19843–19866, 1998. ISSN 2156-2202. doi: 10.1029/97JE03370. URL
1130 <https://agupubs.onlinelibrary.wiley.com/doi/abs/10.1029/97JE03370>. _eprint:
1131 <https://agupubs.onlinelibrary.wiley.com/doi/pdf/10.1029/97JE03370>.
- 1132 F. M. Neubauer, H. Backes, M. K. Dougherty, A. Wennmacher, C. T. Russell,
1133 A. Coates, D. Young, N. Achilleos, N. André, C. S. Arridge, C. Bertucci, G. H.
1134 Jones, K. K. Khurana, T. Knetter, A. Law, G. R. Lewis, and J. Saur. Titan’s
1135 near magnetotail from magnetic field and electron plasma observations and
1136 modeling: Cassini flybys TA, TB, and T3. *Journal of Geophysical Research:
1137 Space Physics*, 111(A10), 2006. ISSN 2156-2202. doi: 10.1029/2006JA011676.
1138 URL <https://onlinelibrary.wiley.com/doi/abs/10.1029/2006JA011676>. _eprint:
1139 <https://onlinelibrary.wiley.com/doi/pdf/10.1029/2006JA011676>.
- 1140 I. Pagano, A. F. Lanza, G. Leto, S. Messina, P. Barge, and A. Baglin. CoRoT-2a
1141 Magnetic Activity: Hints for Possible Star–Planet Interaction. *Earth, Moon, and
1142 Planets*, 105(2):373–378, Sept. 2009. ISSN 1573-0794. doi: 10.1007/s11038-
1143 009-9301-3. URL <https://doi.org/10.1007/s11038-009-9301-3>.
- 1144 J. H. Piddington and J. F. Drake. Electrodynamical Effects of Jupiter’s Satellite Io.
1145 *Nature*, 217:935–+, Mar. 1968.
- 1146 D. H. Pontius. The Io current wing. *Journal of Geophys-
1147 ical Research: Space Physics*, 107(A8):SMP 6–1–SMP 6–12,
1148 2002. ISSN 2156-2202. doi: 10.1029/2001JA000331. URL
1149 <https://agupubs.onlinelibrary.wiley.com/doi/abs/10.1029/2001JA000331>.
- 1150 C. C. Porco, P. Helfenstein, P. C. Thomas, A. P. Ingersoll, J. Wisdom, R. West,
1151 G. Neukum, T. Denk, R. Wagner, T. Roatsch, S. Kieffer, E. Turtle, A. McEwen,
1152 T. V. Johnson, J. Rathbun, J. Veverka, D. Wilson, J. Perry, J. Spitale,
1153 A. Brahic, J. A. Burns, A. D. DelGenio, L. Dones, C. D. Murray, and
1154 S. Squyres. Cassini Observes the Active South Pole of Enceladus. *Sci-
1155 ence*, 311(5766):1393–1401, Mar. 2006. doi: 10.1126/science.1123013. URL
1156 <https://www.science.org/doi/full/10.1126/science.1123013>. Publisher: American
1157 Association for the Advancement of Science.
- 1158 R. Prangé, D. Rego, D. Southwood, P. Zarka, S. Miller, and W. Ip. Rapid energy
1159 dissipation and variability of the Io–Jupiter electrodynamic circuit. *Nature*, 379
1160 (6563):323–325, Jan. 1996. ISSN 1476-4687. doi: 10.1038/379323a0. URL
1161 <https://www.nature.com/articles/379323a0>.
- 1162 W. R. Pryor, A. M. Rymer, D. G. Mitchell, T. W. Hill, D. T. Young, J. Saur, G. H.
1163 Jones, S. Jacobsen, S. W. H. Cowley, B. H. Mauk, A. J. Coates, J. Gustin,
1164 D. Grodent, J.-C. Gérard, L. Lamy, J. D. Nichols, S. M. Krimigis, L. W. Es-
1165 positto, M. K. Dougherty, A. J. Jouchoux, A. I. F. Stewart, W. E. McClintock,
1166 G. M. Holsclaw, J. M. Ajello, J. E. Colwell, A. R. Hendrix, F. J. Crary, J. T.
1167 Clarke, and X. Zhou. The auroral footprint of Enceladus on Saturn. *Nature*, 472
1168 (7343):331–333, Apr. 2011. ISSN 1476-4687. doi: 10.1038/nature09928. URL
1169 <https://www.nature.com/articles/nature09928>.

- 1170 J. Queinnec and P. Zarka. Io-controlled decameter arcs and Io-Jupiter
1171 interaction. *Journal of Geophysical Research: Space Physics*, 103
1172 (A11):26649–26666, 1998. ISSN 2156-2202. doi: 10.1029/98JA02435.
1173 URL <https://onlinelibrary.wiley.com/doi/abs/10.1029/98JA02435>.
1174 _eprint: <https://onlinelibrary.wiley.com/doi/pdf/10.1029/98JA02435>.
- 1175 A. J. Ridley. Alfvén wings at Earth’s magnetosphere under strong in-
1176 terplanetary magnetic fields. *Annales Geophysicae*, 25(2):533–542, Mar.
1177 2007. ISSN 0992-7689. doi: 10.5194/angeo-25-533-2007. URL
1178 <https://angeo.copernicus.org/articles/25/533/2007/>. Publisher: Copernicus
1179 GmbH.
- 1180 L. Roth, J. Saur, K. D. Retherford, D. F. Strobel, P. D. Feldman, M. A. McGrath, and
1181 F. Nimmo. Transient Water Vapor at Europa’s South Pole. *Science*, 343(6167):
1182 171–174, Jan. 2014. ISSN 0036-8075, 1095-9203. doi: 10.1126/science.1247051.
1183 URL <https://science.sciencemag.org/content/343/6167/171>. Publisher: American
1184 Association for the Advancement of Science Section: Report.
- 1185 L. Roth, J. Alday, T. M. Becker, N. Ivchenko, and K. D. Retherford. Detection
1186 of a hydrogen corona at Callisto. *Journal of Geophysical Research: Plan-
1187 ets*, 122(5):1046–1055, 2017. ISSN 2169-9100. doi: 10.1002/2017JE005294.
1188 URL <https://onlinelibrary.wiley.com/doi/abs/10.1002/2017JE005294>.
1189 _eprint: <https://onlinelibrary.wiley.com/doi/pdf/10.1002/2017JE005294>.
- 1190 A. M. Rymer, H. T. Smith, A. Wellbrock, A. J. Coates, and D. T.
1191 Young. Discrete classification and electron energy spectra of Ti-
1192 tan’s varied magnetospheric environment. *Geophysical Research Let-
1193 ters*, 36(15), 2009. ISSN 1944-8007. doi: 10.1029/2009GL039427.
1194 URL <https://onlinelibrary.wiley.com/doi/abs/10.1029/2009GL039427>.
1195 _eprint: <https://onlinelibrary.wiley.com/doi/pdf/10.1029/2009GL039427>.
- 1196 M. Sarantos and J. A. Slavin. On the possible formation of Alfvén wings at
1197 Mercury during encounters with coronal mass ejections. *Geophysical Re-
1198 search Letters*, 36(4), 2009. ISSN 1944-8007. doi: 10.1029/2008GL036747.
1199 URL <https://onlinelibrary.wiley.com/doi/abs/10.1029/2008GL036747>.
1200 _eprint: <https://onlinelibrary.wiley.com/doi/pdf/10.1029/2008GL036747>.
- 1201 J. Saur. A model of Io’s local electric field for a combined Alfvénic and unipolar
1202 inductor far-field coupling. *J. Geophys. Res.*, 109(A18):1210–+, Jan. 2004. doi:
1203 10.1029/2002JA009354.
- J. Saur. Electromagnetic Coupling in Star-Planet Systems. In H. J. Deeg and J. A.
Belmonte, editors, *Handbook of Exoplanets*, pages 1877–1893. Springer Interna-
tional Publishing, Cham, 2018. ISBN 978-3-319-55333-7. doi: 10.1007/978-3-
319-55333-7_7. URL https://doi.org/10.1007/978-3-319-55333-7_7.
- 1204 J. Saur. Overview of Moon–Magnetosphere Interactions. In *Magnetospheres
1205 in the Solar System*, pages 575–593. American Geophysical Union (AGU),
1206 2021. ISBN 978-1-119-81562-4. doi: 10.1002/9781119815624.ch36. URL
1207 <https://onlinelibrary.wiley.com/doi/abs/10.1002/9781119815624.ch36>. Section: 36
1208 _eprint: <https://onlinelibrary.wiley.com/doi/pdf/10.1002/9781119815624.ch36>.
- 1209 J. Saur, F. M. Neubauer, D. F. Strobel, and M. E. Summers. Three-dimensional
1210 plasma simulation of Io’s interaction with the Io plasma torus: Asymmetric

- 1211 plasma flow. *Journal of Geophysical Research: Space Physics*, 104(A11):25105–
 1212 25126, Nov. 1999. ISSN 2156-2202. doi: 10.1029/1999JA900304. URL
 1213 <https://agupubs.onlinelibrary.wiley.com/doi/abs/10.1029/1999JA900304>.
- 1214 J. Saur, T. Grambusch, S. Duling, F. M. Neubauer, and S. Simon. Magnetic energy
 1215 fluxes in sub-Alfvénic planet star and moon planet interactions. *Astronomy & As-*
 1216 *trophysics*, 552:A119, Apr. 2013. ISSN 0004-6361, 1432-0746. doi: 10.1051/0004-
 1217 6361/201118179. URL [https://www.aanda.org/articles/aa/abs/2013/04/aa18179-](https://www.aanda.org/articles/aa/abs/2013/04/aa18179-11/aa18179-11.html)
 1218 [11/aa18179-11.html](https://www.aanda.org/articles/aa/abs/2013/04/aa18179-11/aa18179-11.html).
- 1219 N. Schilling, F. M. Neubauer, and J. Saur. Influence of the internally induced mag-
 1220 netic field on the plasma interaction of Europa. *Journal of Geophysical Research:*
 1221 *Space Physics*, 113(A3), 2008. ISSN 2156-2202. doi: 10.1029/2007JA012842.
 1222 URL <https://onlinelibrary.wiley.com/doi/abs/10.1029/2007JA012842>.
 1223 [_eprint:
 https://onlinelibrary.wiley.com/doi/pdf/10.1029/2007JA012842](https://onlinelibrary.wiley.com/doi/pdf/10.1029/2007JA012842).
- 1224 E. Shkolnik, G. A. H. Walker, and D. A. Bohlender. Evidence for Planet-induced
 1225 Chromospheric Activity on HD 179949. *The Astrophysical Journal*, 597(2):1092–
 1226 1096, Nov. 2003. ISSN 0004-637X. doi: 10.1086/378583. URL
 1227 <https://iopscience.iop.org/article/10.1086/378583>. Publisher: IOP Publishing.
- 1228 E. Shkolnik, D. A. Bohlender, G. A. H. Walker, and A. C. Cameron. The
 1229 On/Off Nature of Star-Planet Interactions*. *The Astrophysical Journal*, 676
 1230 (1):628, Mar. 2008. ISSN 0004-637X. doi: 10.1086/527351. URL
<https://iopscience.iop.org/article/10.1086/527351/meta>. Publisher: IOP Publishing.
- E. L. Shkolnik and J. Llama. Signatures of Star-Planet Interactions. In H. J. Deeg
 and J. A. Belmonte, editors, *Handbook of Exoplanets*, pages 1737–1753. Springer
 International Publishing, Cham, 2018. ISBN 978-3-319-55333-7. doi: 10.1007/978-
 3-319-55333-7_20. URL https://doi.org/10.1007/978-3-319-55333-7_20.
- 1231 I. Sillanpää and R. E. Johnson. The role of ion-neutral collisions in Ti-
 1232 tan’s magnetospheric interaction. *Planetary and Space Science*, 108:73–
 1233 86, Apr. 2015. ISSN 0032-0633. doi: 10.1016/j.pss.2015.01.007. URL
 1234 <https://www.sciencedirect.com/science/article/pii/S0032063315000082>.
- 1235 I. Sillanpää, E. Kallio, R. Jarvinen, and P. Janhunen. Oxygen ions
 1236 at Titan’s exobase in a Voyager 1-type interaction from a hybrid
 1237 simulation. *Journal of Geophysical Research: Space Physics*, 112
 1238 (A12), 2007. ISSN 2156-2202. doi: 10.1029/2007JA012348. URL
 1239 <https://onlinelibrary.wiley.com/doi/abs/10.1029/2007JA012348>.
 1240 [_eprint:
 https://onlinelibrary.wiley.com/doi/pdf/10.1029/2007JA012348](https://onlinelibrary.wiley.com/doi/pdf/10.1029/2007JA012348).
- 1241 S. Simon, A. Wennmacher, F. M. Neubauer, C. L. Bertucci, H. Kriegel,
 1242 J. Saur, C. T. Russell, and M. K. Dougherty. Titan’s highly dynamic
 1243 magnetic environment: A systematic survey of Cassini magnetometer obser-
 1244 vations from flybys TA–T62. *Planetary and Space Science*, 58(10):1230–
 1245 1251, Aug. 2010. ISSN 0032-0633. doi: 10.1016/j.pss.2010.04.021. URL
 1246 <https://www.sciencedirect.com/science/article/pii/S0032063310001339>.
- 1247 S. Simon, J. Saur, H. Kriegel, F. M. Neubauer, U. Motschmann, and M. K.
 1248 Dougherty. Influence of negatively charged plume grains and hemisphere cou-
 1249 pling currents on the structure of Enceladus’ Alfvén wings: Analytical model-
 1250 ing of Cassini magnetometer observations. *Journal of Geophysical Research:*
 1251 *Space Physics*, 116(A4), 2011. ISSN 2156-2202. doi: 10.1029/2010JA016338.

- 1252 URL <https://onlinelibrary.wiley.com/doi/abs/10.1029/2010JA016338>. _eprint:
1253 <https://onlinelibrary.wiley.com/doi/pdf/10.1029/2010JA016338>.
- 1254 S. Simon, H. Kriegel, J. Saur, A. Wennmacher, F. M. Neubauer, E. Rous-
1255 sos, U. Motschmann, and M. K. Dougherty. Analysis of Cassini magnetic
1256 field observations over the poles of Rhea. *Journal of Geophysical Research:*
1257 *Space Physics*, 117(A7), 2012. ISSN 2156-2202. doi: 10.1029/2012JA017747.
1258 URL <https://onlinelibrary.wiley.com/doi/abs/10.1029/2012JA017747>. _eprint:
1259 <https://onlinelibrary.wiley.com/doi/pdf/10.1029/2012JA017747>.
- 1260 S. Simon, P. Addison, and L. Liuzzo. Formation of a Displaced Plasma Wake
1261 at Neptune’s Moon Triton. *Journal of Geophysical Research: Space Physics*,
1262 127(1):e2021JA029958, 2022. ISSN 2169-9402. doi: 10.1029/2021JA029958.
1263 URL <https://onlinelibrary.wiley.com/doi/abs/10.1029/2021JA029958>. _eprint:
1264 <https://onlinelibrary.wiley.com/doi/pdf/10.1029/2021JA029958>.
- 1265 D. Snowden, R. V. Yelle, M. Galand, A. J. Coates, A. Wellbrock,
1266 G. H. Jones, and P. Lavvas. Auroral electron precipitation and flux
1267 tube erosion in Titan’s upper atmosphere. *Icarus*, 226(1):186–204, Sept.
1268 2013. ISSN 0019-1035. doi: 10.1016/j.icarus.2013.05.021. URL
1269 <https://www.sciencedirect.com/science/article/pii/S0019103513002212>.
- A. Strugarek. Models of Star-Planet Magnetic Interaction. In H. J. Deeg and J. A. Bel-
monte, editors, *Handbook of Exoplanets*, pages 1833–1855. Springer International
Publishing, Cham, 2018. ISBN 978-3-319-55333-7. doi: 10.1007/978-3-319-55333-
7_25. URL https://doi.org/10.1007/978-3-319-55333-7_25.
- 1270 A. H. Sulaiman, W. S. Kurth, G. B. Hospodarsky, T. F. Averkamp, S.-
1271 Y. Ye, J. D. Menietti, W. M. Farrell, D. A. Gurnett, A. M. Persoon,
1272 M. K. Dougherty, and G. J. Hunt. Enceladus Auroral Hiss Emissions Dur-
1273 ing Cassini’s Grand Finale. *Geophysical Research Letters*, 45(15):7347–
1274 7353, 2018. ISSN 1944-8007. doi: 10.1029/2018GL078130. URL
1275 <https://agupubs.onlinelibrary.wiley.com/doi/abs/10.1029/2018GL078130>. _eprint:
1276 <https://agupubs.onlinelibrary.wiley.com/doi/pdf/10.1029/2018GL078130>.
- 1277 A. H. Sulaiman, G. B. Hospodarsky, S. S. Elliott, W. S. Kurth, D. A. Gurnett, M. Imai,
1278 F. Allegrini, B. Bonfond, G. Clark, J. E. P. Connerney, R. W. Ebert, D. J. Gershman,
1279 V. Hue, S. Janser, S. Kotsiaros, C. Paranicas, O. Santolík, J. Saur, J. R. Szalay, and S. J.
1280 Bolton. Wave-particle interactions associated with Io’s auroral footprint: Evidence of
1281 Alfvén, ion cyclotron, and whistler modes. *Geophysical Research Letters*, n/a(n/a):
1282 e2020GL088432, 2020. ISSN 1944-8007. doi: 10.1029/2020GL088432. URL
1283 <https://agupubs.onlinelibrary.wiley.com/doi/abs/10.1029/2020GL088432>. _eprint:
1284 <https://agupubs.onlinelibrary.wiley.com/doi/pdf/10.1029/2020GL088432>.
- 1285 A. H. Sulaiman, J. R. Szalay, G. Clark, F. Allegrini, F. Bagenal, M. J. Brennan,
1286 J. E. P. Connerney, V. Hue, W. S. Kurth, R. L. Lysak, J. D. Nichols, J. Saur,
1287 and S. J. Bolton. Poynting Fluxes, Field-Aligned Current Densities, and the Effi-
1288 ciency of the Io-Jupiter Electrodynamical Interaction. *Geophysical Research Letters*,
1289 50(10):e2023GL103456, 2023. ISSN 1944-8007. doi: 10.1029/2023GL103456.
1290 URL <https://onlinelibrary.wiley.com/doi/abs/10.1029/2023GL103456>. _eprint:
1291 <https://onlinelibrary.wiley.com/doi/pdf/10.1029/2023GL103456>.

- 1292 J. R. Szalay, B. Bonfond, F. Allegrini, F. Bagenal, S. Bolton, G. Clark, J. E. P. Con-
 1293 nerney, R. W. Ebert, R. E. Ergun, G. R. Gladstone, D. Grodent, G. B. Hospo-
 1294 darsky, V. Hue, W. S. Kurth, S. Kotsiaros, S. M. Levin, P. Louarn, B. Mauk, D. J.
 1295 McComas, J. Saur, P. W. Valek, and R. J. Wilson. In Situ Observations Con-
 1296 nected to the Io Footprint Tail Aurora. *Journal of Geophysical Research: Planets*,
 1297 123(11):3061–3077, 2018. ISSN 2169-9100. doi: 10.1029/2018JE005752. URL
 1298 <https://agupubs.onlinelibrary.wiley.com/doi/abs/10.1029/2018JE005752>.
- 1299 J. R. Szalay, F. Allegrini, F. Bagenal, S. J. Bolton, B. Bonfond, G. Clark, J. E. P. Conner-
 1300 ney, R. W. Ebert, D. J. Gershman, R. S. Giles, G. R. Gladstone, T. Greathouse, G. B.
 1301 Hospodarsky, M. Imai, W. S. Kurth, S. Kotsiaros, P. Louarn, D. J. McComas, J. Saur,
 1302 A. H. Sulaiman, and R. J. Wilson. Alfvénic Acceleration Sustains Ganymede’s
 1303 Footprint Tail Aurora. *Geophysical Research Letters*, 47(3):e2019GL086527,
 1304 2020a. ISSN 1944-8007. doi: <https://doi.org/10.1029/2019GL086527>. URL
 1305 <https://agupubs.onlinelibrary.wiley.com/doi/abs/10.1029/2019GL086527>. _eprint:
 1306 <https://agupubs.onlinelibrary.wiley.com/doi/pdf/10.1029/2019GL086527>.
- 1307 J. R. Szalay, F. Allegrini, F. Bagenal, S. J. Bolton, B. Bonfond, G. Clark,
 1308 J. E. P. Connerney, R. W. Ebert, V. Hue, D. J. McComas, J. Saur, A. H.
 1309 Sulaiman, and R. J. Wilson. A New Framework to Explain Changes in
 1310 Io’s Footprint Tail Electron Fluxes. *Geophysical Research Letters*, 47(18):
 1311 e2020GL089267, 2020b. ISSN 1944-8007. doi: 10.1029/2020GL089267.
 1312 URL <https://onlinelibrary.wiley.com/doi/abs/10.1029/2020GL089267>. _eprint:
 1313 <https://onlinelibrary.wiley.com/doi/pdf/10.1029/2020GL089267>.
- 1314 J. R. Szalay, F. Bagenal, F. Allegrini, B. Bonfond, G. Clark, J. E. P. Connerney,
 1315 F. Crary, R. W. Ebert, R. E. Ergun, D. J. Gershman, P. C. Hinton, M. Imai,
 1316 S. Janser, D. J. McComas, C. Paranicas, J. Saur, A. H. Sulaiman, M. F. Thom-
 1317 sen, R. J. Wilson, S. Bolton, and S. M. Levin. Proton Acceleration by Io’s
 1318 Alfvénic Interaction. *Journal of Geophysical Research: Space Physics*, 125(1):
 1319 e2019JA027314, 2020c. ISSN 2169-9402. doi: 10.1029/2019JA027314. URL
 1320 <https://agupubs.onlinelibrary.wiley.com/doi/abs/10.1029/2019JA027314>. _eprint:
 1321 <https://agupubs.onlinelibrary.wiley.com/doi/pdf/10.1029/2019JA027314>.
- 1322 A. R. Vasavada, A. H. Bouchez, A. P. Ingersoll, B. Little, C. D. Anger, and The Galileo
 1323 SSI Team. Jupiter’s visible aurora and Io footprint. *J. Geophys. Res.*, 104:27133–+,
 1324 Nov. 1999.
- 1325 V. M. Vasyliūnas. Physical origin of pickup currents. *Annales Geophysicae*, 34(1):
 1326 153–156, Feb. 2016. ISSN 0992-7689. doi: 10.5194/angeo-34-153-2016. URL
 1327 <https://angeo.copernicus.org/articles/34/153/2016/>. Publisher: Copernicus GmbH.
- 1328 G. Viswanath, M. Narang, P. Manoj, B. Mathew, and S. S. Kartha. A Statistical
 1329 Search for Star-Planet Interaction in the Ultraviolet Using GALEX. *The Astro-*
 1330 *nomical Journal*, 159:194, May 2020. ISSN 0004-6256. doi: 10.3847/1538-
 1331 3881/ab7d3b. URL <https://ui.adsabs.harvard.edu/abs/2020AJ....159..194V>. ADS
 1332 Bibcode: 2020AJ....159..194V.
- 1333 G. A. H. Walker, B. Croll, J. M. Matthews, R. Kuschnig, D. Huber, W. W. Weiss,
 1334 E. Shkolnik, S. M. Rucinski, D. B. Guenther, A. F. J. Moffat, and D. Sasselov. MOST
 1335 detects variability on Bootis A possibly induced by its planetary companion. *As-*
 1336 *tronomy and Astrophysics*, 482:691–697, 2008. doi: 10.1051/0004-6361:20078952.

- 1337 S. Wannawichian, J. T. Clarke, and D. H. Pontius. Interaction evidence between Ence-
1338 ladus' atmosphere and Saturn's magnetosphere. *Journal of Geophysical Research:*
1339 *Space Physics*, 113(A7), 2008. ISSN 2156-2202. doi: 10.1029/2007JA012899. URL
1340 <https://agupubs.onlinelibrary.wiley.com/doi/abs/10.1029/2007JA012899>.
- 1341 D. L. Webster, A. Y. Alksne, and R. C. Whitten. Does Io's Ionosphere Influence Jupiter's
1342 Radio Bursts? *The Astrophysical Journal*, 174:685, June 1972. ISSN 0004-637X.
1343 doi: 10.1086/151530. URL <https://ui.adsabs.harvard.edu/abs/1972ApJ...174..685W>.
1344 ADS Bibcode: 1972ApJ...174..685W.
- 1345 H. Y. Wei, C. T. Russell, J.-E. Wahlund, M. K. Dougherty, C. Bertucci, R. Modolo, Y. J.
1346 Ma, and F. M. Neubauer. Cold ionospheric plasma in Titan's magnetotail. *Geophys-*
1347 *ical Research Letters*, 34(24), 2007. ISSN 1944-8007. doi: 10.1029/2007GL030701.
1348 URL <https://onlinelibrary.wiley.com/doi/abs/10.1029/2007GL030701>.
1349 _eprint: <https://onlinelibrary.wiley.com/doi/pdf/10.1029/2007GL030701>.
- 1350 D. J. Williams and B. Mauk. Pitch angle diffusion at Jupiter's moon
1351 Ganymede. *Journal of Geophysical Research: Space Physics*, 102
1352 (A11):24283–24287, 1997. ISSN 2156-2202. doi: 10.1029/97JA02260.
1353 URL <https://onlinelibrary.wiley.com/doi/abs/10.1029/97JA02260>.
1354 _eprint: <https://onlinelibrary.wiley.com/doi/pdf/10.1029/97JA02260>.
- 1355 D. J. Williams and R. M. Thorne. Energetic particles over Io's po-
1356 lar caps. *Journal of Geophysical Research: Space Physics*, 108
1357 (A11), 2003. ISSN 2156-2202. doi: 10.1029/2003JA009980. URL
1358 <https://agupubs.onlinelibrary.wiley.com/doi/abs/10.1029/2003JA009980>.
- 1359 D. J. Williams, B. H. Mauk, R. E. McEntire, E. C. Roelof, T. P. Armstrong, B. Wilken,
1360 J. G. Roederer, S. M. Krimigis, T. A. Fritz, and L. J. Lanzerotti. Electron Beams and
1361 Ion Composition Measured at Io and in Its Torus. *Science*, 274:401–403, Oct. 1996.
- 1362 D. J. Williams, B. Mauk, and R. W. McEntire. Trapped electrons in
1363 Ganymede's magnetic field. *Geophysical Research Letters*, 24(23):
1364 2953–2956, 1997a. ISSN 1944-8007. doi: 10.1029/97GL03003.
1365 URL <https://onlinelibrary.wiley.com/doi/abs/10.1029/97GL03003>.
1366 _eprint: <https://onlinelibrary.wiley.com/doi/pdf/10.1029/97GL03003>.
- 1367 D. J. Williams, B. H. Mauk, R. W. McEntire, E. C. Roelof, T. P. Armstrong,
1368 B. Wilken, J. G. Roederer, S. M. Krimigis, T. A. Fritz, L. J. Lanze-
1369 rotti, and N. Murphy. Energetic particle signatures at Ganymede: Im-
1370 plications for Ganymede's magnetic field. *Geophysical Research Letters*,
1371 24(17):2163–2166, 1997b. ISSN 1944-8007. doi: 10.1029/97GL01931.
1372 URL <https://onlinelibrary.wiley.com/doi/abs/10.1029/97GL01931>.
1373 _eprint: <https://onlinelibrary.wiley.com/doi/pdf/10.1029/97GL01931>.
- 1374 A. N. Wright. The interaction of Io's Alfvén waves with the Jovian mag-
1375 netosphere. *Journal of Geophysical Research: Space Physics*, 92(A9):
1376 9963–9970, 1987. ISSN 2156-2202. doi: 10.1029/JA092iA09p09963. URL
1377 <https://agupubs.onlinelibrary.wiley.com/doi/abs/10.1029/JA092iA09p09963>.
1378 _eprint: <https://agupubs.onlinelibrary.wiley.com/doi/pdf/10.1029/JA092iA09p09963>.
- 1379 A. N. Wright and D. J. Southwood. Stationary Alfvénic structures. *J. Geophys. Res.*,
1380 92:1167–1175, 1987.

- 1381 P. Zarka. Auroral radio emissions at the outer planets: Observations
1382 and theories. *Journal of Geophysical Research: Planets*, 103(E9):20159–
1383 20194, Aug. 1998. ISSN 0148-0227. doi: 10.1029/98JE01323. URL
1384 <https://agupubs.onlinelibrary.wiley.com/doi/abs/10.1029/98JE01323>.
- 1385 H. Zhang, K. K. Khurana, M. G. Kivelson, S. Fatemi, M. Holmström, V. An-
1386 gelopoulos, Y. D. Jia, W. X. Wan, L. B. Liu, Y. D. Chen, H. J. Le,
1387 Q. Q. Shi, and W. L. Liu. Alfvén wings in the lunar wake: The role
1388 of pressure gradients. *Journal of Geophysical Research: Space Physics*, 121
1389 (11):10,698–10,711, 2016. ISSN 2169-9402. doi: 10.1002/2016JA022360.
1390 URL <https://onlinelibrary.wiley.com/doi/abs/10.1002/2016JA022360>. eprint:
1391 <https://onlinelibrary.wiley.com/doi/pdf/10.1002/2016JA022360>.
- 1392 H. Zhou, G. Tóth, X. Jia, and Y. Chen. Reconnection-Driven Dynamics at
1393 Ganymede’s Upstream Magnetosphere: 3-D Global Hall MHD and MHD-EPIC Sim-
1394 ulations. *Journal of Geophysical Research: Space Physics*, 125(8):e2020JA028162,
1395 2020. ISSN 2169-9402. doi: <https://doi.org/10.1029/2020JA028162>. URL
1396 <https://agupubs.onlinelibrary.wiley.com/doi/abs/10.1029/2020JA028162>. eprint:
1397 <https://agupubs.onlinelibrary.wiley.com/doi/pdf/10.1029/2020JA028162>.
- 1398 C. Zimmer, K. K. Khurana, and M. G. Kivelson. Subsurface Oceans on Europa
1399 and Callisto: Constraints from Galileo Magnetometer Observations. *Icarus*, 147
1400 (2):329–347, Oct. 2000. ISSN 0019-1035. doi: 10.1006/icar.2000.6456. URL
1401 <https://www.sciencedirect.com/science/article/pii/S001910350096456X>.

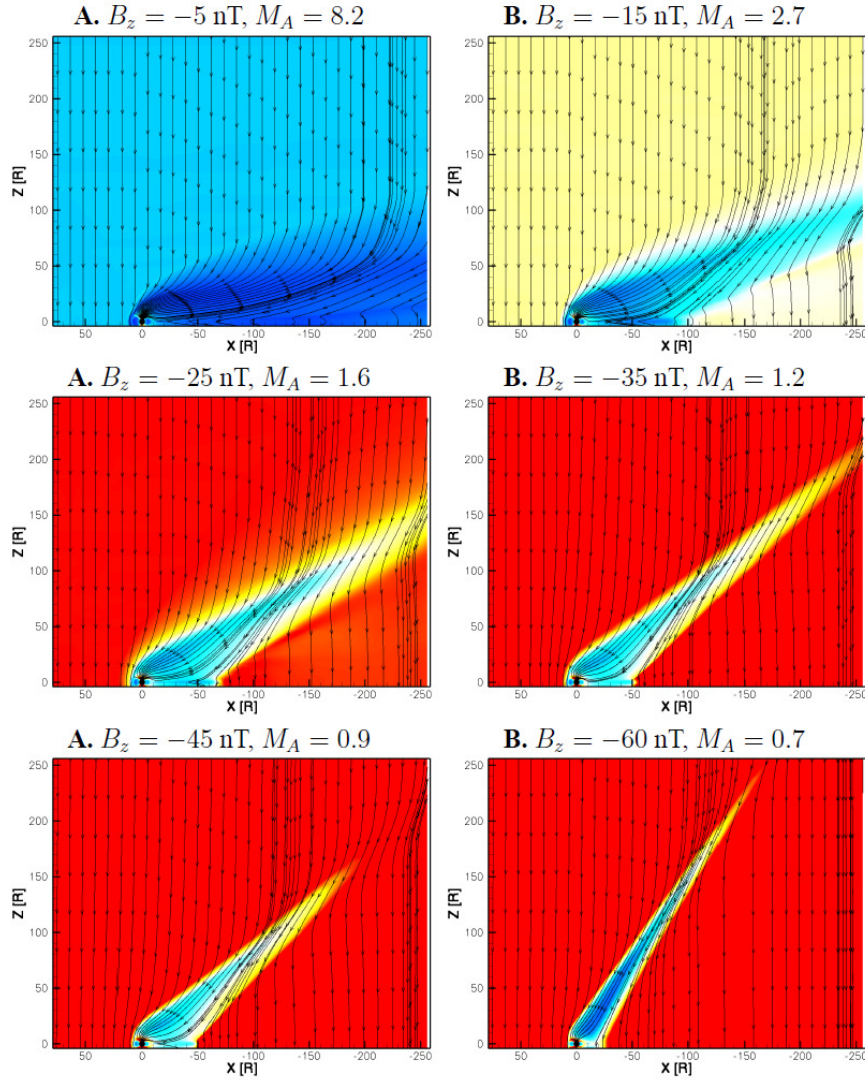


Fig. 1 Outputs from magneto-hydrodynamic simulations of the interaction between the solar wind and the Earth. The colors represent the electric field (dark blue is 0 mV/m and red is 10 mV/m) and the lines represent the magnetic field. Images of the velocity fields would display similar features. Starting from typical conditions and a Alfvén Mach number (M_A) of 8.2, we can see that the magnetotail transforms progressively into Alfvén wings as the M_A decreases. When Alfvén wings form, energy and currents can be efficiently carried away from the interaction site over long distances. From Ridley (2007).

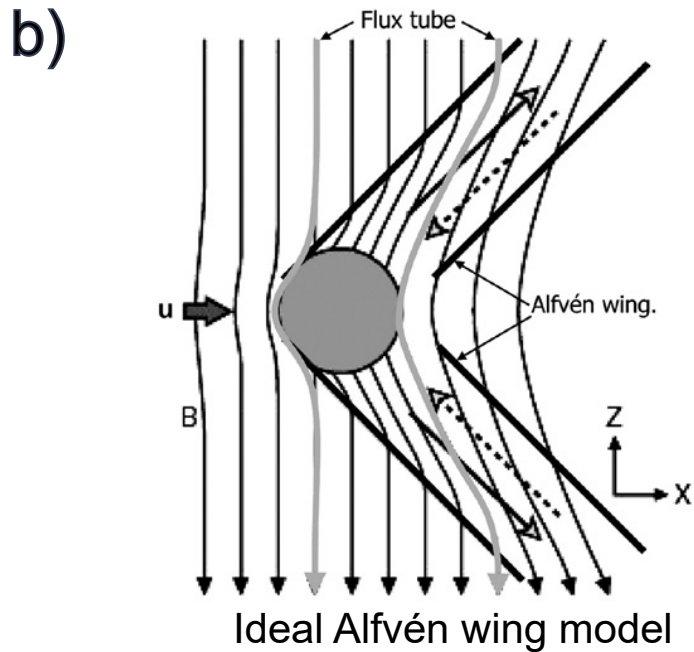
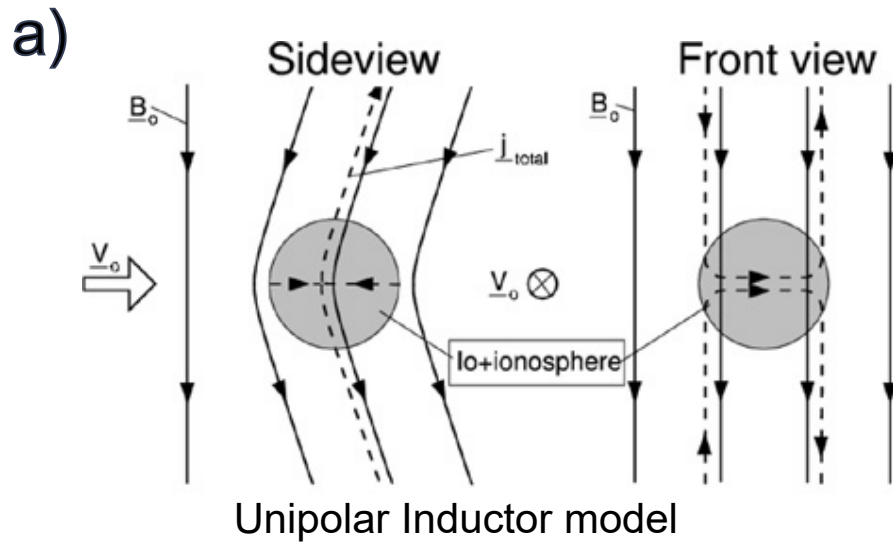


Fig. 2 (Top) Schematic of the local interaction in the case of immediate feedback from the planet's ionosphere to the moon (the "unipolar inductor"). (Bottom) Schematic of the local interaction in the case where there is no feedback from the planet's ionosphere to the moon (the "ideal Alfvén wing model"). In the first case, the Io flux tube and the Alfvén wing are identical, while in the second, they are decoupled. Adapted from Saur (2004) and Kivelson et al. (2004).

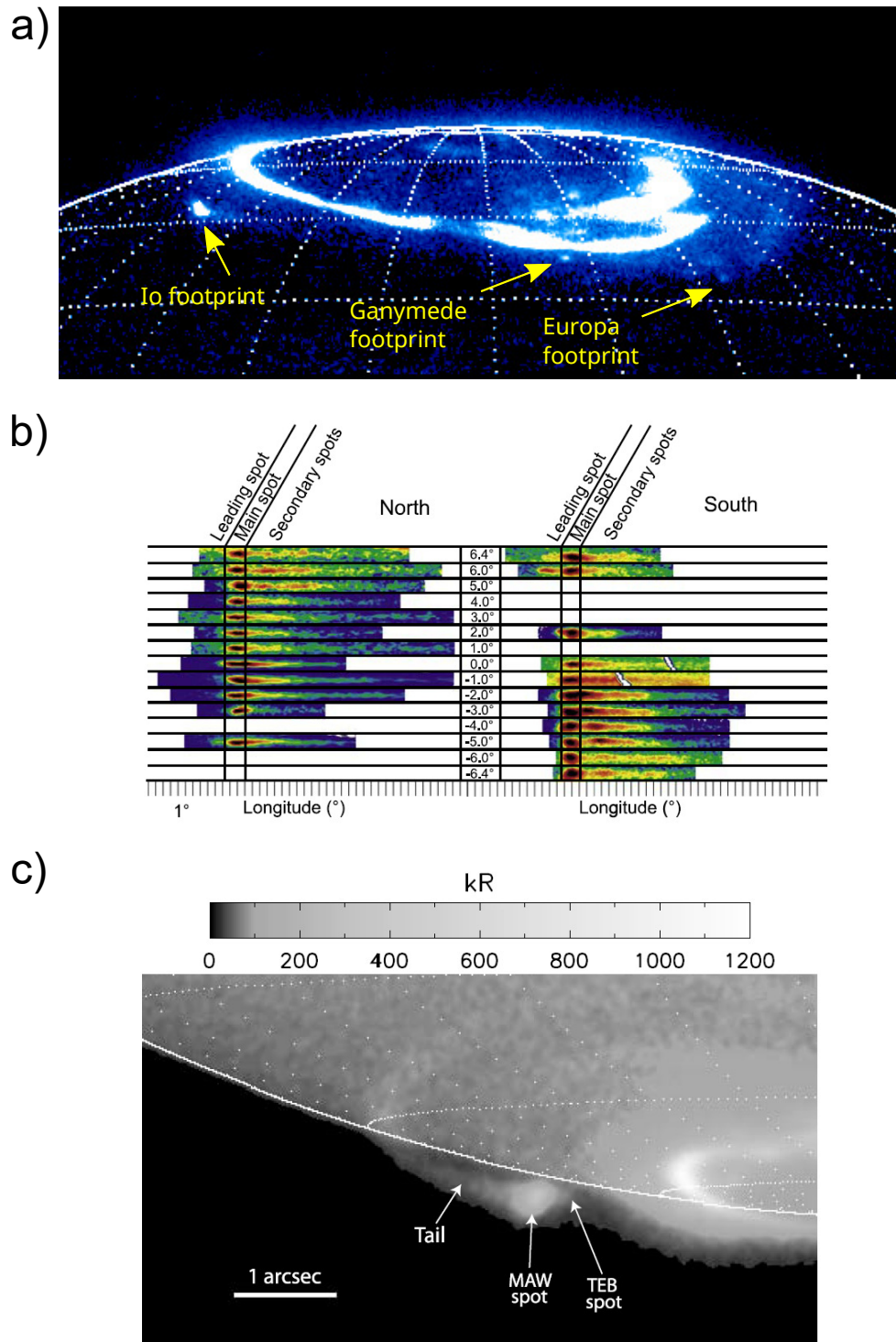


Fig. 3 a) Image of the northern FUV aurora of Jupiter acquired with the Hubble Space Telescope’s ACS camera on 7 February 2006. The Io, Europa, and Ganymede footprints are simultaneously visible. Adapted from Bonfond (2012). b) Scheme of the Io morphology as a function of the centrifugal latitude of Io in the torus. The longitudes are not measured on the planet, but mapped to the equatorial plane along the magnetic field lines according to the VIP4 magnetic field model for an easier comparison of both hemispheres. Adapted from Bonfond et al. (2008). c) Example of Io footprint tail and spots observed above the limb. Adapted from Bonfond (2010).

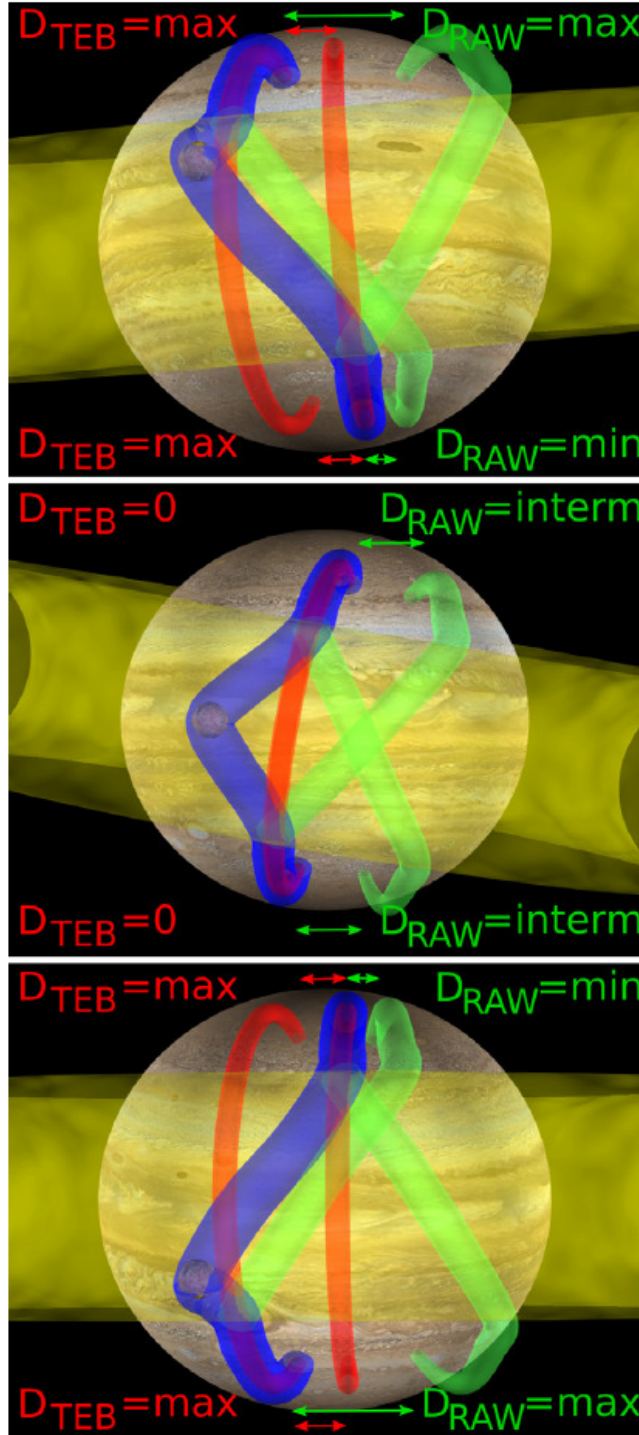


Fig. 4 Schematic of the Alfvén wing reflection pattern and Trans-hemispheric Electron Beams (TEB, shown in red) when Io is in its northern-most (top), central (middle) or southern-most position relative to the plasma torus (shown in yellow). The Main Alfvén Wing (MAW) is shown in blue and the reflected Alfvén wing (RAW) is shown in green. On the top panel, in the North, the distance between the MAW spot and the TEB spot (D_{TEB}) is maximal as well as the distance between the MAW spot and the RAW spot (D_{RAW}). Note that in a linear case, $\max(D_{RAW}) \sim 2\max(D_{TEB})$. In the South, D_{TEB} is also maximal, but the TEB spot is now upstream of the MAW spot. D_{RAW} reaches its minimum. When Io is in the center of the torus (middle panel) the situation in the two hemispheres is symmetric, and the TEB spots are merged with the MAW spots. Adapted from (Bonfond et al., 2017b).

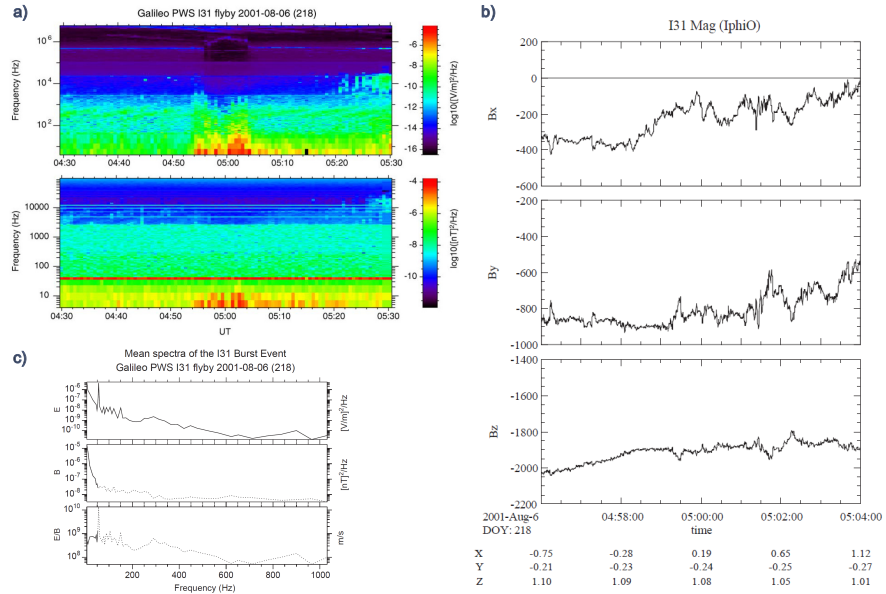


Fig. 5 a) Calibrated dynamic spectra of the electric field (top) and magnetic field (bottom) acquired by the PWS (Plasma Wave Subsystem) instrument on board Galileo during the I31 flyby on 7 December 1995. The Alfvén wing crossing started about 5 minutes before the closest approach (04:59:20)

b) Magnetic field observations during the crossing of the Alfvén wings during the same event, but the time interval is narrowed down to the duration of the Alfvén wing crossing. The x-axis is parallel to the unperturbed flow, the y-axis is pointing towards Jupiter and the z-axis is parallel to Jupiter’s rotation axis. c) Electric and magnetic wave spectra, and the corresponding ratio of these two quantities. In this example, it can be seen that the crossing of the Alfvén wing is accompanied with the observation of intense higher frequency waves (with most of the energy remaining below 50 Hz), which have been interpreted as the signature of turbulent filamentation of the Alfvén waves originating from Io. Adapted from Chust et al. (2005).

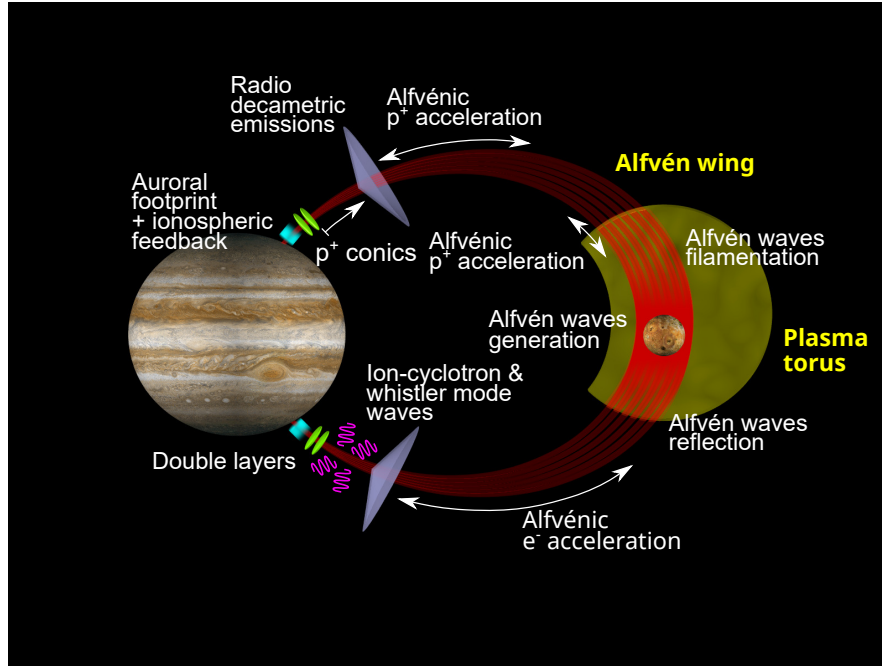


Fig. 6 Schematic of the chain of processes arising from the Io-Jupiter electromagnetic interaction.

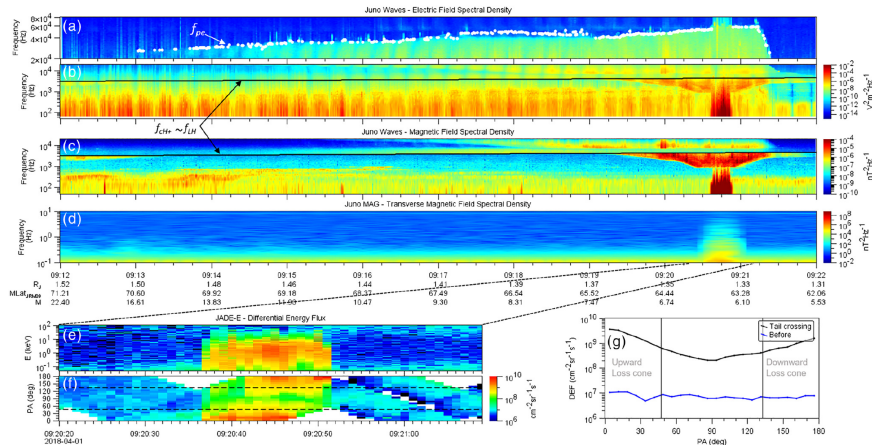


Fig. 7 (a-d) Electric and magnetic field frequency-time spectrograms measured in the MAW revealing MHD and plasma waves across multiple scales, namely, Alfvén, ion cyclotron, and whistler modes. (e-g) Electron data revealing broadband and bidirectional distributions of electrons, likely accelerated by inertial Alfvén waves at the high latitudes, and also the source of whistler-mode waves. (From Sulaiman et al. (2020))

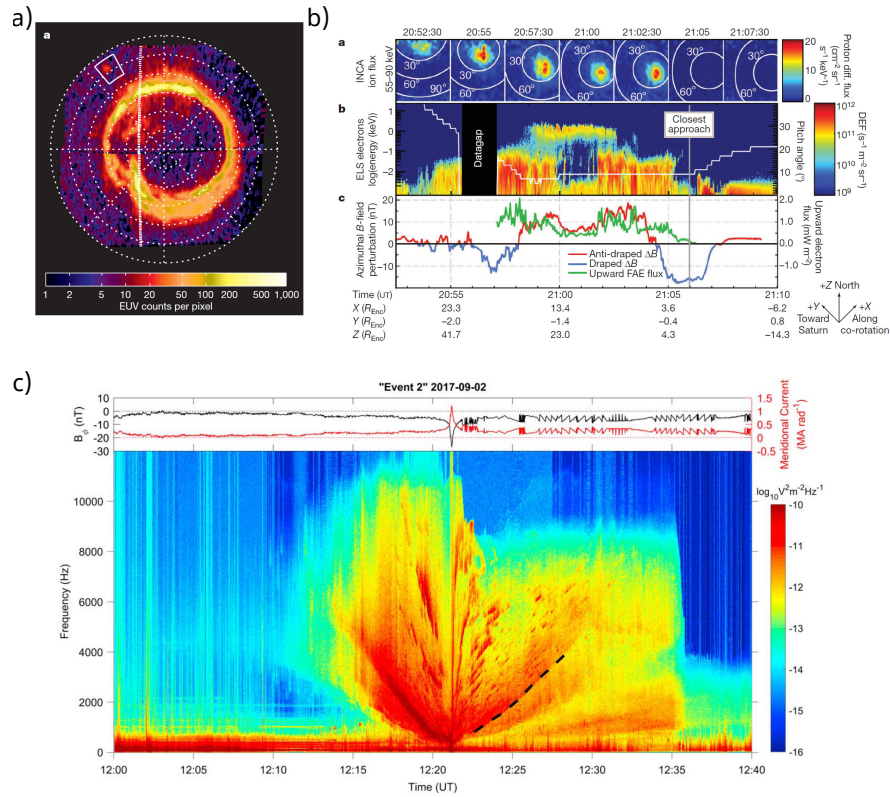


Fig. 8 a) Image of the Extreme-UV northern aurora at Saturn acquired on 26 August 2008 by the UltraViolet Imaging Spectrograph on board Cassini. The spot highlighted on the top left side is the Enceladus footprint. b) Particle and field measurements acquired around the 11 August 2008 flyby of Enceladus by Cassini's Ion and Neutral Camera (INCA), Electron Spectrometer (ELS) and magnetometer. The observed ion and electron beams are originating from Saturn's north pole and were thus accelerated close to the planet and away from it, reminiscent of the electron beams creating the TEB spots at Jupiter. c) High-resolution electric field dynamic spectrogram of the auroral hiss emissions as Cassini was crossing the Enceladus Alfvén wing at high latitude on 2 September 2017. A ray tracing analysis indicates that the source region is co-located with the Enceladus footprint on Saturn. a) and b) are from Pryor et al. (2011), c) is from Sulaiman et al. (2018).

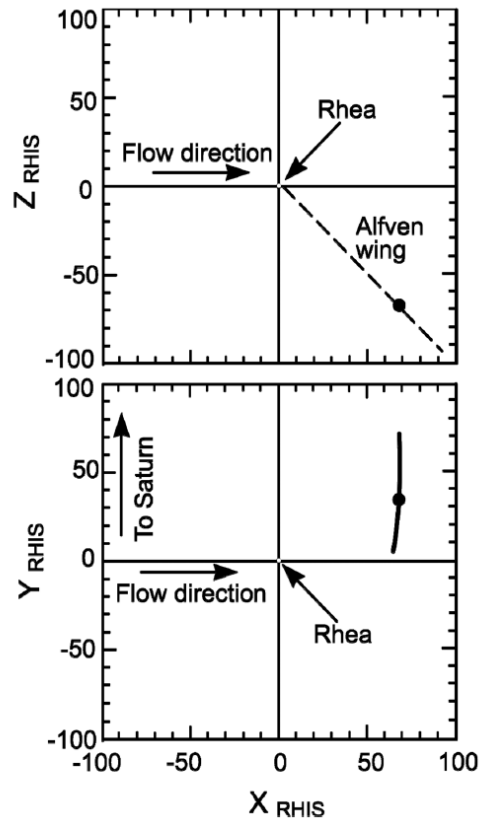


Fig. 9 Plot of the Cassini trajectory during the distant Rhea encounter of 3 June 2010. The black circle marks the passage through the Alfvén wing. Tracing the Alfvén waves back in time (dashed lines) shows that they originate from Rhea or its close wake. From (Khurana et al., 2017).

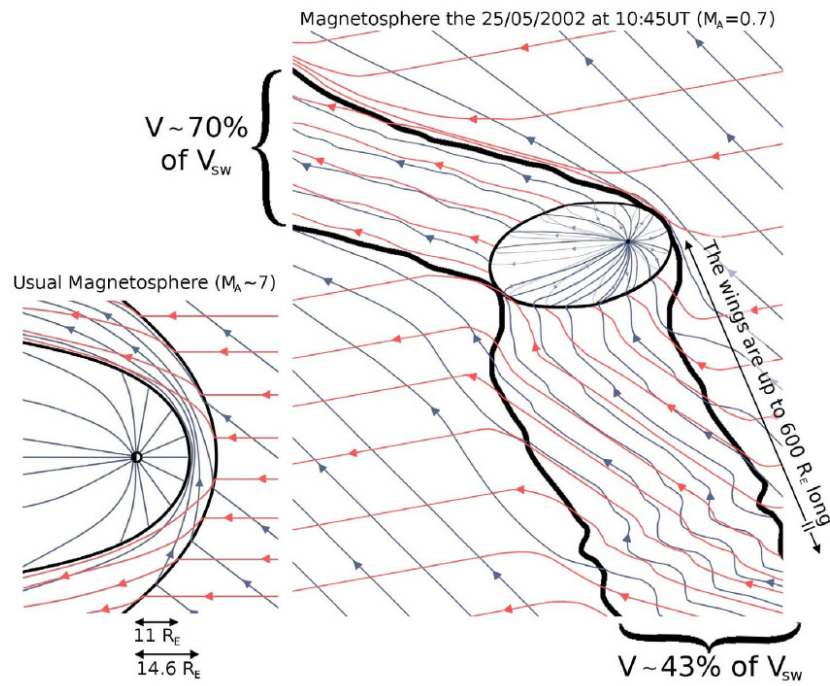


Fig. 10 Sketches of the interaction between the solar wind and the Earth's magnetosphere seen from the north. The magnetic field is shown in blue, the velocity in red. The left sketch shows the typical configuration of the magnetosphere while the right one shows the development of Alfvén wings at a time during which the interplanetary medium density at Earth dropped so much that the Alfvén mach number was below one. The Geotail spacecraft was located on the dusk side of the Earth (i.e. towards the top of the image) and entered and exited from the Alfvén wing several times. From Chané et al. (2012)

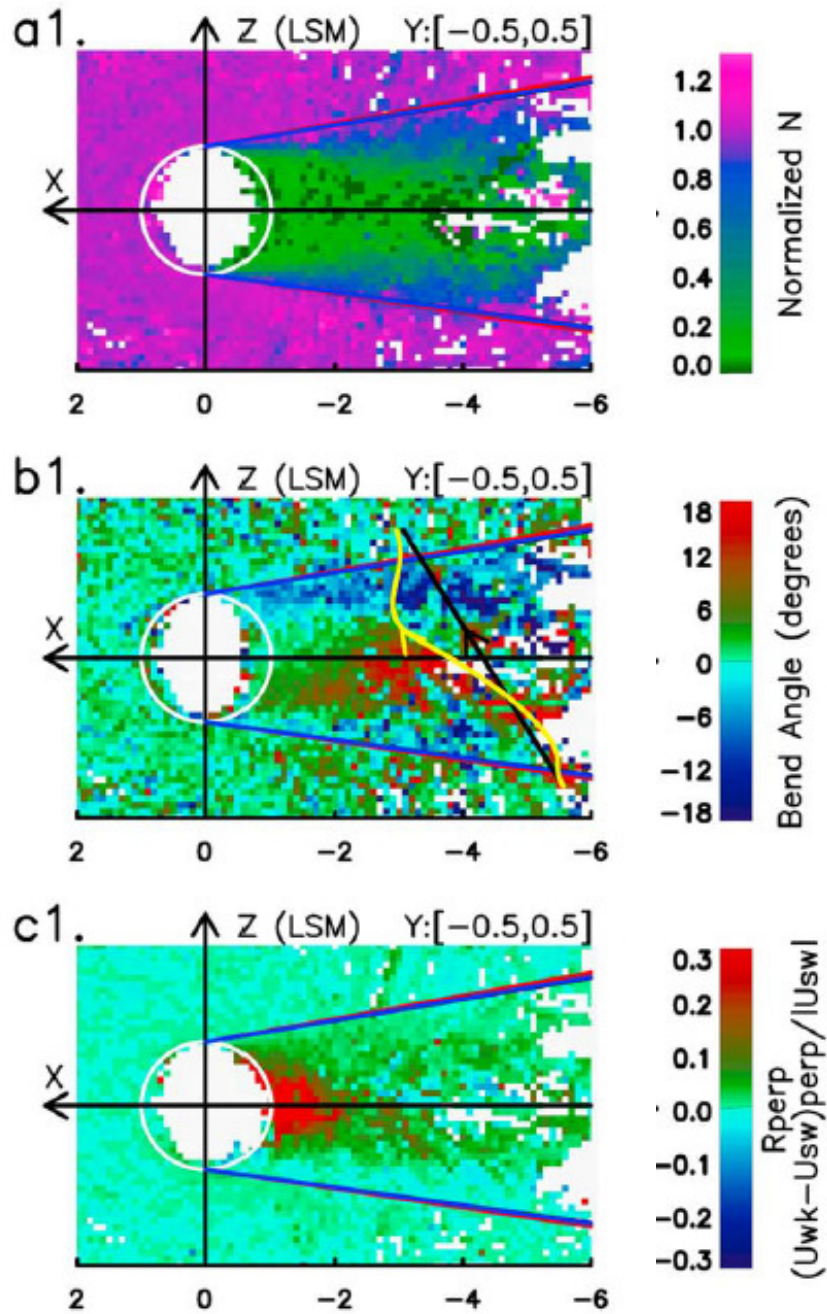


Fig. 11 Distribution of the average ARTEMIS measurements for the density normalized by the ion density in the solar wind (top), the bent angle of the magnetic field magnetic δ_{XZ} (middle) and the X component of the plasma flow deceleration rate in the Moon's wake (bottom). The density gradient stemming from the absorption of the plasma by the Moon's surface is the source of Alfvén wings, which manifest through a deceleration of the plasma flow and a bending of the magnetic field in the wake. Adapted from Zhang et al. (2016).